INVESTIGATION OF RADIO-FREQUENCY MIXING IN A HELIUM MAGNETOMETER

STANLEY A. HERMAN

INVESTIGATION OF RADIOFREQUENCY MIXING IN A HELIUM MAGNETOMETER

* * * *

Stanley A. Herman

INVESTIGATION OF RADIOFREQUENCY MIXING IN A HELIUM MAGNETOMETER

by

Stanley A. Herman
//
Major, United States Marine Corps

Submitted in partial fulfillment of
the requirements for the degree of

MASTER OF SCIENCE
IN
ENGINEERING ELECTRONICS

United States Naval Postgraduate School
Monterey, California

1962

INVESTIGATION OF RADIOFREQUENCY MIXING IN A HELIUM MAGNETOMETER

by

Stanley A. Herman

This work is accepted as fulfilling
the thesis requirements for the degree of
MASTER OF SCIENCE
IN
ENGINEERING ELECTRONICS
from the
United States Naval Postgraduate School

ABSTRACT

Any spin system can be used as a mixer for two radiofrequency driving fields if the two frequencies of these fields are both near the resonance frequency. The purpose of this paper is to investigate the phase change of the difference frequency in the vicinity of the Larmor frequency in a helium magnetometer. The theories of optical pumping and radiofrequency mixing are presented. These are followed by a description of the experimental apparatus and procedure and a presentation of the results. From the results, it appears that a helium magnetometer can be constructed as a closed loop oscillator.

The writer's work in this investigation was accomplished at the Varian Associates research laboratory at Palo Alto, California, during the period January to March 1962.

The writer wishes to express his appreciation for the assistance and encouragement given him by Dr. James T. Arnold of Varian Associates in this investigation.

The writer also wishes to thank Professors Carl E. Menneken and Eugene C. Crittenden, Jr. of the U. S. Naval Postgraduate School for their constructive criticism in the preparation of this paper.

TABLE OF CONTENTS

LIST OF ILLUSTRATIONS

I. Introduction

One of the most important applications of optical pumping has been the precise measurement of weak magnetic fields. To this end, several magnetometer systems have been developed using either alkali metal vapor or triplet metastable helium as the r-f resonant element. A number of these devices are currently in use for measurement of the geomagnetic field at or near the surface of the earth.

The basic theory around which all of these instruments are designed was presented by Dehmelt[1] and Bloom and Bell.[2] All of these systems share the following apparatus in common: a bright source producing an intense collimated beam of radiation, a circular polarizer, an absorption cell containing the vapor to be optically pumped, a radiofrequency coil to produce resonance in the pumped vapor, and a photocell to monitor the transmitted light.

The change in optical transmission of the spin system upon application of a resonance r-f field depends in detail on the direction of the incident light beam relative to the constant magnetic field. The behavior of the spin system can be described by the three variables M_x, M_y, and M_z of Bloch's equations for a spin system.[3] The signal present at the photocell is proportional to M_n where n is the direction of the light beam relative to the magnetic field.

A second method of utilizing the pumping light involves the principle of "pumping light modulation".[4]

1. H. G. Delmelt, Phys. Rev. 105, 1487, 1924 (1957)
2. W. E. Bell and A. L. Bloom, Phys. Rev. 107, 1559 (1957)
3. F. Bloch, Phys. Rev. 70, 460 (1946)
4. W. E. Bell and A. L. Bloom, Optical Driven Spin Precession, Phys. Rev. Ltrs. 6, 280, (1961)

This method utilizes a polarized pumping light modulated at the appropriate Larmor precession frequency. Passing the light through a helium sample results in a net spin orientation within the gas. The amount of absorption will be altered as the modulation frequency passes through the natural spin precession frequency corresponding to the ambient magnetic field.[5] Detection of this orientation is accomplished by monitoring the pumping light intensity after it passes through a helium absorption cell.

A third method of utilizing the pumping light consists in heterodyning the modulated pumping light frequency and the r-f resonance drive frequency. If the two frequencies are within the line width of the Larmor precession frequency, a difference frequency can be extracted from the light for magnetometer purposes.[6]

A theoretical study and experimental evaluation of this last method dealing with the phase characteristics of the difference frequency in the vicinity of resonance was undertaken with the intent of determining if it were possible to make use of this phase characteristic, possibly in the design of a closed loop oscillator.

In order to present the results of these efforts in a comprehensive manner, this thesis contains a discussion of the helium atom, optical pumping theory and radiofrequency mixing theory. Following this is a description of the experimental apparatus, procedure, and results.

5. R. G. Aldrich, Thesis, U. S. Naval Postgraduate School, Monterey, (1961)
6. A. L. Bloom and W. E. Bell, Radiofrequency Mixing in Optical Pumping Experiments, to be published

II. Theoretical Background

A. Quantum Mechanics of the Helium Atom

Each helium atom contains two electrons. There are, therefore, six coordinates to deal with instead of three. For the purpose of obtaining a general idea of possible states, an exact solution is not necessary. A first approximation to the problem can be treated by neglecting the mutual interaction of the electrons, afterwards, the interaction can be taken into account by the methods of the Theory of Perturbations.

In the absence of an external magnetic field three quantum numbers are associated with each of the two electrons: n_1, ℓ_1, j_1 and n_2, ℓ_2, j_2. In the following discussion assume that ℓ_1 is greater than ℓ_2. The corresponding angular momenta are added vectorially to obtain a total angular momentum, "$J = j_1 + j_2$". Likewise, the total orbital and spin angular moments are given, respectively, by "$L = \ell_1 + \ell_2$" and "$S = s_1 + s_2$".

Assuming that the magnitude of the respective angular momentum vector is proportional to ℓ, s, or j has the advantage that all possible magnitudes of the resultant quantum numbers can be determined easily and quickly. However, this method gives inadequate information regarding the relative directional characteristics of the angular momentum vectors. If directional properties of the vectors are also desired, correct quantum mechanical values of the angular momentum, $\ell^* = [\ell(\ell+1)]^{1/2}$, $L^* = [L(L+1)]^{1/2}$, $s^* = [s(s+1)]^{1/2}$, $S^* = [S(S+1)]^{1/2}$, $j^* = [j(j+1)]^{1/2}$, $J^* = [J(J+1)]^{1/2}$ must be used.

Alignment of the angular momentum vectors in this manner further induces a precession of these vectors around the resultant vector direction

Experimental results show that the coupling relations in helium are normal. That is, the coupling relations are such that the spin vectors and the orbital vectors are added separately into resultant L and S. The vectors ℓ_1 and ℓ_2 rotate about the total orbital moment L, the spin vectors s_1 and s_2 around S, and then these two vectors precess around J. This coupling is known as Russell-Saunders coupling. Figure 1 illustrates how L and S add to give J.

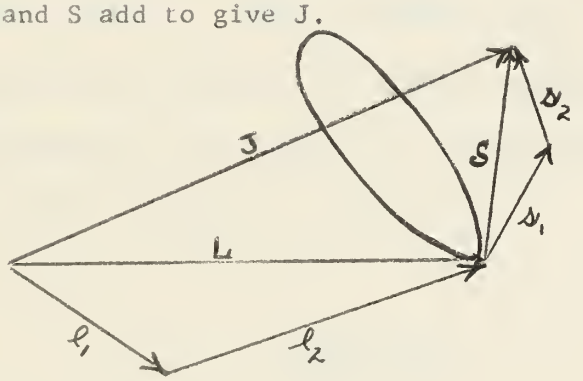

Fig. 1 Russell-Saunders (L-S) Coupling

The two orbital moments ℓ_1 and ℓ_2 are first combined into the total orbital moment, L, which must be a whole number and can take only the values $L = \ell_1 - \ell_2, \ell_1 - \ell_2 + 1, \ldots \ell_1 + \ell_2$. The two spin moments combine into the total spin moment which must be a whole number, since s_1 and s_2 have the value $s = \frac{1}{2}$. Therefore, the only possible values for S are 0 and 1.

The term scheme of helium breaks up into two separate groups, according as the spin is zero or one. The case where S = 0 is called parahelium and when S = 1, orthohelium. This separation of terms into the two groups has been proved experimentally. It can be shown that in general there are no radiative transitions between terms of the first and second group.

In parahelium, the total spin moment S = 0; therefore, J = L. This implies that all of the terms of parahelium are singlets; for every L there is only a single term with J = L.

In orthohelium, the total spin moment is equal to 1, and combines vectorially with the total orbital moment to form the total moment, J. Since all three vectors are whole numbers, J, in this case, can take on the values J = L - 1, L, L + 1. There are three terms for every orbital quantum number, and the term scheme is a triplet system.

The individual terms of the triplet ^3P_J are distinguished by right hand lower indices, which indicate the value of J.

For example:

$^1P_1$	parahelium
$^3P_0$ $^3P_1$ $^3P_2$	orthohelium

In the absence of any external field, the state is specified by n, J, L, and S according to the notation:

$$n\,{}^{2S+1}L_J$$

The first number, denoting the principal quantum number, indicates the "shell" which the electrons occupy. The capital letter indicates the orbital moment S,P,D,... corresponding to the quantum numbers L = 0,1,2,.... The left hand upper index gives the maximum number of terms in the term groups defined by the principal quantum number and the capital letter. It is equal to 2S + 1. The right hand lower index distinguishes the individual terms of this group. It is the total angular momentum, J.

At room temperature unexcited helium atoms essentially lie in the singlet ground state denoted by 1^1S_0. By suitable excitation, the atoms

are raised to the higher singlet and triplet energy levels. In a time of the order of 10^{-8} second the singlet levels radiate down to the $1\ ^1S_0$ level while the triplet levels radiate down to the $2\ ^3S_1$ level, which is the lowest triplet level. The $2\ ^3S_1$ level does not combine with $1\ ^1S_0$ ground state. Those terms which cannot go to a lower state with emission of radiation and, also, cannot be reached from a lower state by absorption are called metastable. Hence, electrons remain excited in this metastable state for relatively long periods of time. The atoms are dependent on collisions with other atoms to decay to the $1\ ^1S_0$ ground state. Perturbations due to the proximity of electric fields of atoms or molecules will also allow the return of the electrons in the metastable states to the ground levels. It is found experimentally that the energy levels of orthohelium corresponding to a given value of n, L ($\neq 0$) and S ($= 1$) are split into three fine structure levels according as $J = L + 1$, L, $L - 1$, with $J = L - 1$ lying highest and the $J = L + 1$ lying lowest in energy.

Fig. 2 shows the fine structure splitting for the $2\ ^3P_J$ levels of helium. The $2\ ^3S_1$ level of helium is not split, since $L = 0$ and $J = S = 1$ only. To summarize, the fine structure splitting represents the dependence of the energy for a given value of n, L, and S on the possible J values.

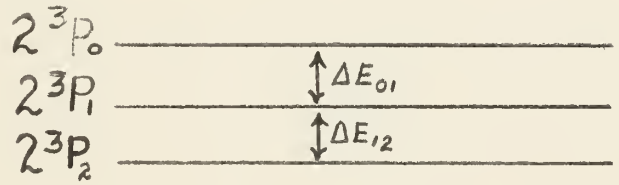

Fig. 2 Fine Structure of $2\ ^3P_J$ Energy Levels

The importance of the fine structure splitting insofar as the helium magnetometer is concerned is as follows: the alignment of the $2\ ^3S_1$ sublevels can take place only if a coherent absorption and incoherent re-emission of the resonance radiation takes place. This in turn is dependent upon the degree of thermal mixing of the $2\ ^3P_J$ levels. Since the fine structure energy difference between these levels is of the order of the average thermal energy of the atom, mixing can take place and incoherent re-emission can take place, thus providing the basis for optical pumping.

B. Larmor's Theorem

If an atom is brought into a homogeneous magnetic field, H, a motion of precession of the orbit plane sets in around the direction of the field. This precession is called the Larmor precession and the relation expressing the frequency of precession is called Larmor's theorem. This theorem states that to a first approximation the change in the motion of an electron about the nucleus produced by the introduction of a magnetic field of intensity H is a precession of the orbit about the field direction with uniform angular velocity:

$$\omega_L = H \cdot \frac{e}{2m}$$

It has been shown classically that, in terms of electron orbits, the ratio between the magnetic moment μ and the orbital angular momentum p is given by $\frac{\mu}{p} = \frac{e}{2m} = \gamma =$ gyromagnetic ratio. Therefore, the angular velocity of the Larmor precession is equal to the field strength H times the gyromagnetic ratio: $\omega_L = \gamma H$

The classical theory shows that, as the magnetic field starts from zero and gradually increases, there is no change in the size or shape of the electron orbit. As the orbit precesses with angular velocity, ω_L, the orbit normal describes a cone about the field direction H.[7]

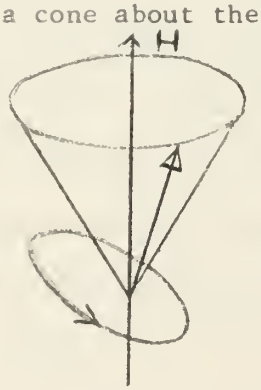

Fig. 3 Larmor Precession

7. Becker, Introduction to Theoretical Mechanics, McGraw Hill Book Co., 1954, Pg. 304

C. The Anomalous Zeeman Effect

The anomalous Zeeman effect is the observed phenomenon that in a weak magnetic field a spectral line is split up into a considerable number of lines. According to classical theory, and wave mechanics when spin is not taken into account, there is only the normal Zeeman effect, that is the splitting of every spectral line into a Lorentz triplet.

The anomalous Zeeman effect can be explained by assuming the magnetic spin-moment is obtained from the mechanical by multiplying by $2^{e}/_{m}$

$$M_s = \frac{2e}{4\pi m} s$$

Since the mechanical spin-moment is always $s = \frac{1}{2}$, the magnetic moment of the electron is exactly equal to a Bohr magneton.

The difference between the orbital and spin moments is responsible for the anomalous Zeeman effect. The result is that the total magnetic moment is not, in general, in the same direction as the total mechanical moment J. The general case for several electrons is shown in Fig. 4. For clearness, M_{ℓ}, the magnetic orbital moment, is shown twice as large as ℓ and M_s, the magnetic spin moment, must be shown four times as large as the mechanical spin moment, s. The resultants M_J and J fall in different directions. In keeping with the meaning of J, the total angular momentum, the atom, together with the whole vector figure, must be rotating about the direction given by J. Any vector not in this direction precesses about it.

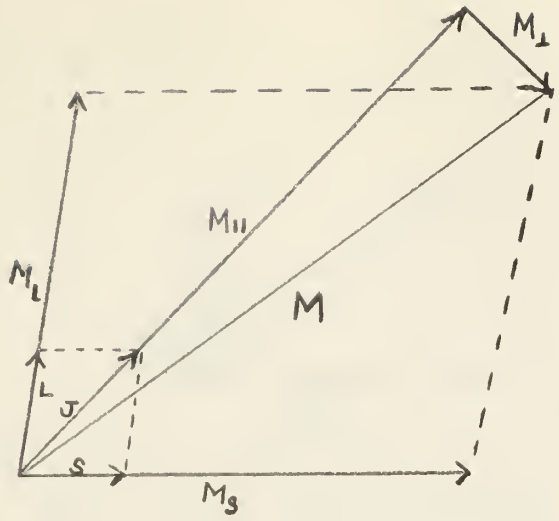

Fig. 4 Vector Model for Anomalous Zeeman Effect

In the presence of a weak external magnetic field the atom possesses an effective magnetic moment, M, in the direction of J. Because of the angular momentum it precesses about the direction of the field. J possesses 2J + 1 possible settings with respect to the field direction, these being characterized by the m component of J in this direction. The magnetic energies of these are given individually by $M_{11}Hm/_J$. The undisturbed term is therefore split by the magnetic field into 2J + 1 terms with separation $M_{11}H/_J$ where $M_{11} = \frac{e}{4\pi m} g$. The factor g gives the divergencies which occur in the vector model.

The additional magnetic energy is then given by

$$E_{mag} = -\frac{M_{11}}{J} H_{mag} = \frac{e}{4\pi m} H_{mag} = -h\nu_L m g$$

Where ν_L = Larmor frequency. The undisturbed term is split up by the magnetic field, into 2J + 1 terms, but the amount of splitting differs by the factor g which is called the Lande splitting factor. It varies from term to term and is the determining cause of the anomalous behavior of the atom in the Zeeman effect.

The splitting up of a line in the anomalous Zeeman effect is essentially determined by the Lande factors for the upper and lower states. This factor can be obtained very simply.

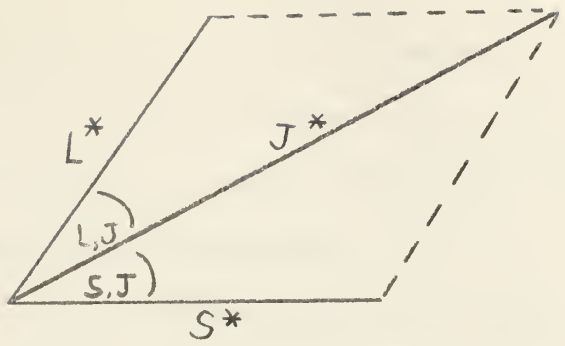

Fig. 5 Vector Composition of J = L + S

$$M_{\parallel} = M_L \cos(L,J) + M_S \cos(S,J)$$

by substitution:

$$\frac{eh}{4\pi m} J^* g = \frac{eh}{4\pi m} \left\{ L^* \cos(L,J) + 2S^* \cos(S,J) \right\}$$

which gives:

$$g = \frac{L^*}{J^*} \cos(L,J) + \frac{2S^*}{J^*} \cos(S,J)$$

solving for the cosines:

$$\cos(L,J) = \frac{(J^*)^2 + (L^*)^2 - (S^*)^2}{2 J^* L^*}$$

$$\cos(S,J) = \frac{(J^*)^2 + (S^*)^2 - (L^*)^2}{2 J^* S^*}$$

therefore:

$$g = 1 + \frac{(J^*)^2 + (S^*)^2 - (L^*)^2}{2(J^*)^2}$$

and finally:

$$g = \frac{3}{2} + \frac{S(S+1) - L(L+1)}{2J(J+1)}$$

The importance of this g-factor cannot be over emphasized, for it gives directly the relative separations of the Zeeman levels for the different terms.

For the $^3S_1$ level of helium, g = 2, while for the ^3P_J levels, g = 3/2.

This corresponds to a frequency splitting of 2.8mc per gauss between adjacent $^3S_1$ Zeeman sublevels and a frequency splitting of 2.1mc per gauss between ^3P_J Zeeman sublevels. This difference in frequency splitting enables one to excite transitions between $^3S_1$ sublevels and not disturb the ^3P_J sublevels.

Relevant energy levels of a helium atom is an external magnetic field are shown in Fig. 6.

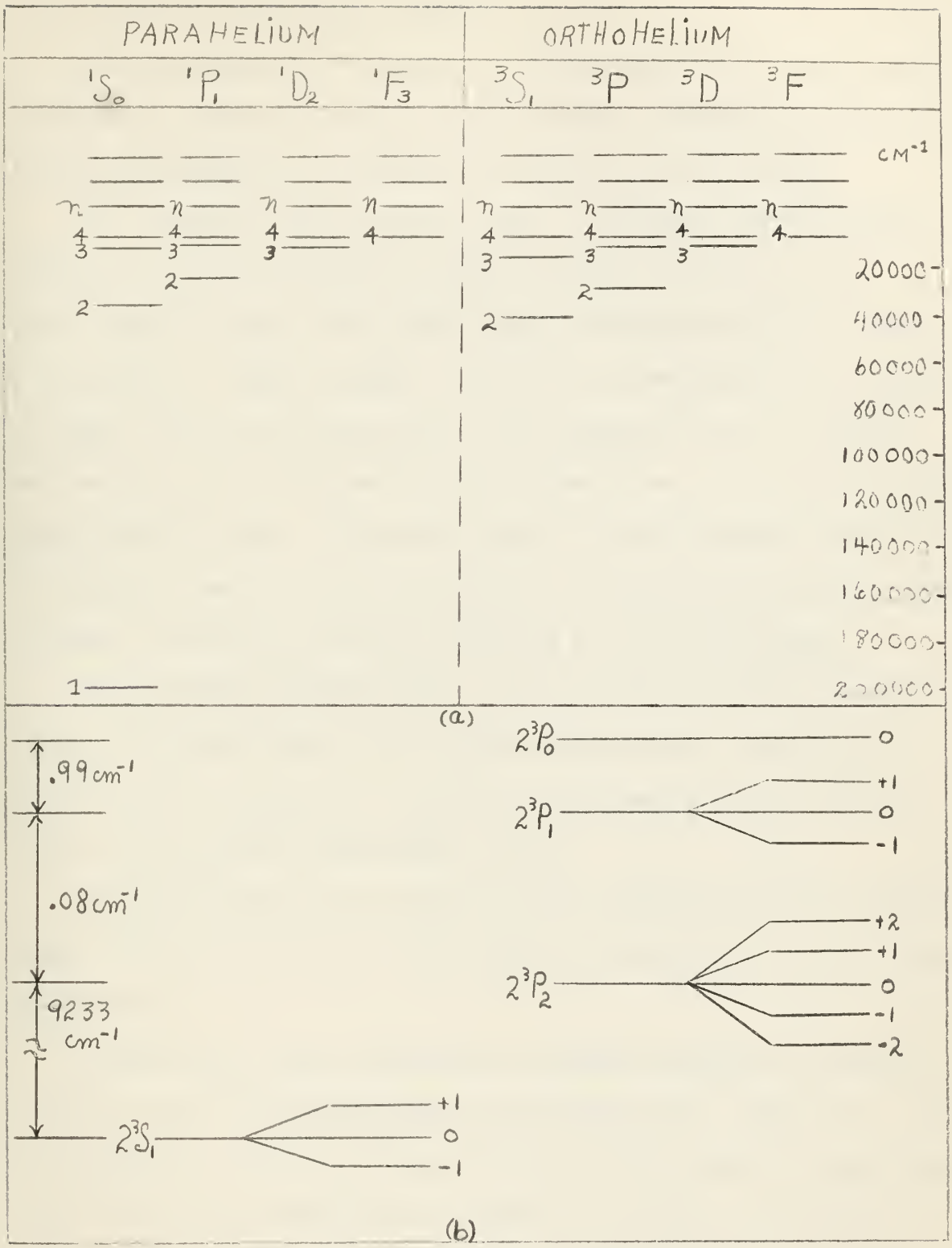

Fig. 6 (a) Energy Levels of Helium (b) Relevant Energy Levels of a Helium Atom in An External Magnetic Field

III. Theory of Basic Optical Pumping

Optical pumping is the process by which individual atoms are raised from lower to higher states of internal energy. The word optical is used because the frequency is in the optical region of the spectrum.

The transition between energy levels is threefold: atoms at higher levels tend to fall spontaneously into the lower one; those at the lower level will jump to the higher one if the required quanta of energy are available. Those in higher level will be stimulated to emit a quantum of energy and go to a lower level. If a transition is to be detected spectroscopically, there must be a net excess either of downward or upward jumps among the atoms. In jumping upward, the atoms subtract photons from a transmitted beam of radiation producing an absorption spectrum; in jumping down, they send out photons, producing an emission spectrum.

In the helium absorption cell, a weak discharge excites some atoms from the $^1S_0$ ground state to the $^3S_1$ metastable state. Decay to the ground state by radiation is forbidden, so helium atoms live in this state for a relatively long period of time.

In a weak magnetic field, the $^3S_1$ state is split into three equally spaced levels. And the three ^3P_J levels are split into 1, 3, and 5 levels respectively.

A bright light from a helium lamp is passed through the absorption cell and excites the helium atoms to the higher levels. There are a total of 18 possible transitions from the $^3S_1$ to the ^3P_J levels for unpolarized light. With the introduction of a circular polarizer, the available transitions are limited to a total of six possibilities of being pumped to the P state. In effect Δm is restricted to + 1 for circular polarized light from the S to the P state. Fig. 7 is a diagrammatic representation of the splitting of the ^3P_J levels in a weak magnetic field and Table 1

is the transition from the S state to the P state with circular polarized light.

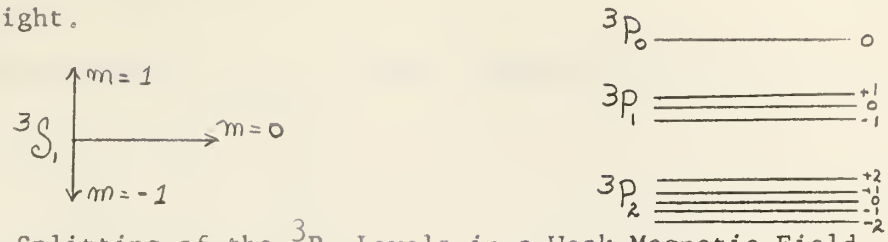

Fig. 7 Splitting of the ^3P_J Levels in a Weak Magnetic Field

		P_0	P_1			P_2					RATIO
		0	+1	0	-1	+2	+1	0	-1	-2	
S_1	+1					X					1
	0		X				X				2
	-1	X		X				X			3

Table 1 Transitions from the S state to the P state with Circular Polarized Light

Therefore, it is assumed that the ratio of pumping probabilities is proportional to (1,2,3) with the (-) state the most likely of being pumped. The following restriction is placed on Δm: $\Delta m = +1$ for transitions to the P state and $\Delta m = \pm 1$ or 0 for incoherent transitions from the P states.

Therefore:

$$\frac{d(+)}{dt} = -\lambda(1)(+) + \frac{N}{3} - \frac{1}{R}\{(+) - (+e)\}$$
$$\frac{d(0)}{dt} = -\lambda(2)(0) + \frac{N}{3} - \frac{1}{R}\{(0) - (0e)\}$$
$$\frac{d(-)}{dt} = -\lambda(3)(-) + \frac{N}{3} - \frac{1}{R}\{(-) - (-e)\}$$

where:

$(+),(0),(-)$ = number of atoms in each of the states

λ = arbitrary constant introduced by the light

$1, 2, 3$ = relative probabilities of being selected

N = to al number of transitions from P states

$\frac{1}{R}\begin{Bmatrix}(+)-(+e)\\(0)-(0e)\\(-)-(-e)\end{Bmatrix}$ = return to equilibrium $\equiv R_+, R_0, R_-$

The quantities leaving and returning to the $^3S_1$ state have to be equal. Consequently, by simple mathematics, $6\lambda = N$

Consider the case where $R_{+,0,-}$ is small compared with λ :

$$\frac{d(+)}{dt} = -1\lambda(+) + 2\lambda - R_+$$
$$\frac{d(0)}{dt} = -2\lambda(0) + 2\lambda - R_0$$
$$\frac{d(-)}{dt} = -3\lambda(-) + 2\lambda - R_-$$

It can be seen from the above equations, that the return from the P state is equally likely to enter any of the S states. But the departure from the S state is most probable in the (-) and least in the (+) state. Consequently, there is a build up in the (+) state. Given enough time every atom must end up in the (+) state and the helium is then pumped to saturation.

A detailed analysis of the effect of polarization on transitions and population density considerations may be found in reference (5).

The pumping can be undone by applying radio-frequency energy to induce transitions between the Zeeman levels. The exact energy and hence the frequency, required to do this depends on the strength of the magnetic field; in a field of one half gauss, typical of earth's magnetism, the frequency at which helium resonates between the $^3S_1$ sublevels is about 1.4 mc/s. Thus the effect of the r-f field is to equalize the populations of the Zeeman sublevels in the absence of other effects. The absorption of resonance radiation produces an inequality of the populations which is dependent upon the orientation of the optical axis with respect to the steady state magnetic field. The effect of the r-f will be to lessen the degree of population difference. For a high enough r-f level the resonance radiation effects become much smaller than the r-f effects, and equal populations result. The most convenient way to observe this resonance is by varying the earth's field a little in recurrent cycles.

Before the field reaches the correct value for the radio frequency the levels are saturated or depleted and little light energy is abstracted from the light beam; transitions are induced when the field reaches resonance and now the populations are redistributed. The brightness of the light drops sharply; the drop registers as a dip in an oscilloscope trace. Consequently, if the frequency is known, the experiment can be used to determine the earth's magnetic field with high accuracy.

A second method is to induce transitions by modulation of the light source. This method also utilizes a polarized pumping light, modulated at the appropriate Larmor precession frequency, to change the population densities of the metastable levels. Light energy pumps the helium atoms to the upper states. The modulating frequency passes through the resonance frequency and redistributes the population densities. Detection is accomplished by monitoring the pumping light intensity after it passes through the absorption cell. The amount of absorption will be altered as the modulating frequency passes through the natural spin precession frequency corresponding to the ambient magnetic field.[8]

The effect in detail is described as follows: If the light beam is oriented perpendicular to the earth's magnetic field, Ho, and no r-f field is applied, the following equations for the spin system are obtained:

$$\frac{dF}{dt} + j\gamma H_o F + \frac{F}{S_2} = P_x \mathcal{M}'$$

$$\frac{dM_z}{dt} + \frac{M_z}{S_1} = 0$$

8. R. G. Adrich, Thesis, U. S. Naval Postgraduate School, Monterey, 1961

where:

$F = M_x + j M_y$

P_x is the pumping rate of the light

S_1, S_2 are relaxation times including effects of light

m' is the equilibrium polarization that would be produced by the light in the absence of the magnetic field and thermal relaxation effects.

Normally, with no modulation, the steady state solution is very small

$$M_z = 0 \quad \therefore F \propto \frac{1}{\gamma H_0}$$

However, let the light be modulated so that

$$P_x = a + b \cos \omega t$$
$$1/S_2 = R + b \cos \omega t$$

then a large steady state solution exists in the form

$$F = \frac{1/2\, b\, m'}{R + j \Delta\omega} e^{-j\omega t}$$

where $\Delta\omega = \gamma H_0 - \omega$

The effect can be observed most easily as a change in average intensity of the transmitted light. The absorption of light by the cell is proportional to $P_x (1 - M_x)$, and the resultant signal in the photocell is then proportional to

$$- \frac{1/4\, R b^2 m'}{R^2 + \Delta\omega^2} + (\text{terms at } \omega \text{ and } 2\omega)$$

which represents a secular increase in the transmitted light at resonance.

If the system is considered to be in a coordinate system rotating at, ω, the "rotating" lamp is turned on only in a certain preferred direction, it is effectively stationary in a frame of reference in which the effective magnetic field is very weak. An analysis of the rotating coordinate system will be found in the following section. Optical pumping then will take place as if the effective field were parallel to the light beam.[9]

9. W. E. Bell and A. L. Bloom, Phys. Rev. Ltrs., 6, 280 (1961)

IV. Theory of Radio Frequency Mixing of Pulsed Light and R - F Magnetic Resonance Frequencies

Any spin system can be used as a mixer for two radio frequency driving fields if the frequencies of these fields are both near the resonant frequency.

In the following discussion the two driving frequencies are respectively, the pulsed light frequency, ω_2, and the r-f magnetic drive frequency, ω_1; the best S/N ratio for the pulsed light is when the light beam and the magnetic field are at right angles to each other, while the best signal from the r-f drive is when the light beam and the magnetic field are parallel. Consequently, the best signal obtainable from both of them is a compromise and should be at an orientation in which the light beam is at approximately a 45 degree angle to the magnetic field.

In this section Bloch's equations will be used for the magnetic and thermal description. Each atom is considered to have a magnetic moment, $\vec{\mu}$ and an intrinsic angular momentum, $\vec{a}$. The magnetic moment $\vec{\mu}$ will be either parallel or anti-parallel to $\vec{a}$ so that $\vec{\mu} = \gamma \vec{a}$, where γ is the gyromagnetic ratio which is taken positive when $\vec{\mu}$ and $\vec{a}$ are parallel as is the case with a classical positive rotating charge and negative when $\vec{\mu}$ and $\vec{a}$ are anti-parallel.

The resultant macroscopic magnetization can be represented by the magnetization vector $\vec{M}$. The resultant macroscopic angular momentum, $\vec{A}$ and the magnetization $\vec{M}$ are related by $\vec{M} = \gamma \vec{A}$. The rate of change of $\vec{A}$ is classically equal to the torque, $\vec{T}$, acting on the system $\frac{d\vec{A}}{dt} = \vec{T}$.

The torque on a dipole $\vec{M}$ placed in a magnetic field $\vec{H}$ is $\vec{T} = \vec{M} \times \vec{H}$. Replacing $\vec{A}$ by $\frac{\vec{M}}{\gamma}$ we have the equation of motion, $\frac{d\vec{M}}{dt} = \gamma(\vec{M} \times \vec{H})$,

of the magnetization vector in the presence of a magnetic field. The magnetic field will ordinarily consist of a strong steady magnetic field along the z-axis, a weak oscillating field along the x-axis and certain weak random internal fields which shall be neglected for the present.

The components of $\vec{H}$ are therefore:

$H_x = 2H_1 \cos \omega t$

$H_y = 0$

$H_z = Ho$

A solution of $\frac{d\vec{M}}{dt} = \gamma(\vec{M} \times \vec{H})$ is desired under the condition that ω of the impressed field is close to the Larmor frequency, $\omega_L = \gamma H_o$.

It is convenient to transform $\frac{d\vec{M}}{dt} = \gamma(\vec{M} \times \vec{H})$ from the fixed coordinate system to one rotating about the z-axis with angular frequency ω. A rotating coordinate system will be presented.[10] This may be done by using the following general vector equation to relate change in the fixed coordinate system $\frac{d\vec{V}}{dt}$ to rate of change in the rotating system $\frac{D\vec{V}}{dt}$:

$$\frac{d\vec{V}}{dt} = \frac{D\vec{V}}{dt} + \vec{\omega} \times \vec{V}$$

Substitute $\vec{M}$ for $\vec{V}$ and use the equation of motion of the magnetic vector in the presence of a magnetic field $\frac{d\vec{M}}{dt} = \gamma(\vec{M} \times \vec{H})$

$$\frac{D\vec{M}}{dt} = -\vec{\omega} \times \vec{H} + \gamma \vec{M} \times \vec{H} = \gamma(\vec{M} \times \vec{\omega}/\gamma + \vec{M} \times \vec{H})$$

$$\frac{d\vec{M}}{dt} = \gamma \vec{M}' \times \vec{H}_{eff}$$ where the prime indicates that $\vec{M}$ is in the rotating frame.

10. M. Packard, The Method of Nuclear Induction, Thesis, 1949

H_{eff} gives the effective field imposed in the rotating frame as is defined: $\vec{H}_{eff} = \vec{H} + \vec{\omega}/\gamma$ with $\vec{H}$ and $\vec{\omega}$ measured in the stationary system.

If the new system is chosen to rotate around the z-axis with a circular frequency, ω, the following equations will transform the coordinates from the fixed to the rotating system:

$$X = X' \cos \omega t + Y' \sin \omega t$$

$$Y = -X' \sin \omega t + Y' \cos \omega t$$

$$Z = Z'$$

and from the rotating coordinate system to the fixed system by:

$$X' = X \cos \omega t - Y \sin \omega t$$

$$Y' = X \sin \omega t + Y \cos \omega t$$

$$Z' = Z$$

where $\gamma > 0$

The components of the magnetic field will transform like the above coordinates: H_{eff} can be transformed easily to the rotating frame.

The effective magnetic field in the rotating system is:

$$H_{x'} = H_1 + H_1 \cos 2\omega t$$

$$H_{y'} = -H_1 \sin 2\omega t$$

$$H_{z'} = H_0 - \omega/\gamma$$

The x' and y' components of the magnetic field represent two fields; one is fixed along the x' axis and the other is a rotating field which appears to rotate at 2 ω. It has been shown by Bloch and Siegert (1940) that to the order $(H1/Ho)^2$ the rotating part of this field can be ignored, leaving

$$H_{x1} = H_1$$

$$H_{y'} = 0$$

$$H_{z'} = H_0 - \omega/\gamma 1$$

where $H_{x1}^2 + H_{z1}^2 = \overline{H}_{ass}^2$

The equations of motion of $\vec{M}'$ with the above magnetic field are easily found:

$$\frac{dM_{x'}}{dt} = \gamma M_{y'}(H_0 - \omega/\gamma)$$

$$\frac{dM_{y'}}{dt} = \gamma M_{z'}H_1 - \gamma M_{x'}(H_0 - \omega/\gamma)$$

$$\frac{dM_{z'}}{dt} = -\gamma M_{y'}H_1$$

The random weak internal fields which are actually present, but have so far been neglected, can be considered to affect the electron system in essentially two ways:

First by contributing to a change in the energy of the total spin system proportional to $M_{z'}$ and second by affecting the relative phase of the individual electrons in their precession about the z' axis, and therefore the $M_{x'}$ and $M_{y'}$ components of the total polarization vector.

The component which lies near ω of the Fourier spectrum of the random fields will induce energy transfer from the spin system to thermal motion of the surroundings while the low frequency part of the spectrum will produce local fields which alter ω.

If it is assumed, for the case of spin energy transfer, that with no supplied R-F magnetic field the $M_{z'}$ component exponentially approaches the equilibrium value M_0, the rate of change of M_Z' is

$$\frac{dM_{z'}}{dt} = -\frac{(M_{z'} - M_0)}{T_1} \qquad (1)$$

where

T_1 = longitudinal or thermal relaxation time and gives a measure of the time required to establish the equilibrium polarization M_o.

Analogously, the transverse relaxation time T_2 may be introduced which gives the time for the M_x' and M_y' components to decrease by 1/e. Assuming an exponential behavior,

$$\frac{dM_{x'}}{dt} = -\frac{M_{x'}}{T_2} \tag{2}$$

and

$$\frac{dM_{y'}}{dt} = \frac{-M_{y'}}{T_2} \tag{3}$$

Equations 1,2,3 are equations of motion of $\overline{M}'$ in the absence of any applied r-f magnetic field.

If it is assumed that the complete equation of motion is obtained by a simple addition of the rates of change given by these equations and those which govern the motion in the presence of an r-f field, the complete equations of motion are:

$$\frac{dM_{x'}}{dt} = \gamma M_{y'}(H_o - \omega/\gamma) - \frac{M_{x'}}{T_2}$$

$$\frac{dM_{y'}}{dt} = \gamma M_{z'}H_1 - \gamma M_{x'}(H_o - \omega/\gamma) - \frac{M_{y'}}{T_2}$$

$$\frac{dM_{z'}}{dt} = -\gamma M_{y'}H_1 - \frac{(M_{z'} - M_o)}{T_1}$$

From the above equations, which are known as the Bloch equations,[11] the following differential equations, with proper substitutions, can be written:

11. F. Bloch, Phys. Rev. 70, 460 (1946)

$$\frac{dM_{x'}}{dt} = \gamma M_{y'}(H_0 - \omega/\gamma) - \frac{M_{x'}}{S} + \frac{M_{x'}^{(0)}}{S} \tag{4}$$

$$\frac{dM_{y'}}{dt} = \gamma M_{z'}H_1 - \gamma M_{x'}(H_0 - \omega/\gamma) - \frac{M_{y'}}{S} + \frac{M_{y'}^{(0)}}{S} \tag{5}$$

$$\frac{dM_{z'}}{dt} = -\gamma M_{y'}H_1 - \frac{M_{z'}}{S} + \frac{M_{z'}^{(0)}}{S} + \frac{M_0^{(0)}}{T} \tag{6}$$

where

$\frac{M_{x',y',z'}}{S}$ = rate of return to equilibrium, includes optical and thermal processes

$M_{x',y',z'}^{(0)}$ = magnetization in absence of a magnetic field; Optical pumping only

$M_0^{(0)}$ = magnetization in absence of optical pumping; magnetic field only, assumed = 0

$S = S_1 = S_2$ = relaxation times

$S_1 = (P_x + P_y + P_z + T_1^{-1})^{-1}$

$S_2 = (P_x + P_y + P_z + T_2^{-1})^{-1}$

T = real relaxation time in absence of pumping

P_x, P_y, P_z = pumping rates

The H_{eff} vector is rotating about the z-axis at an angular frequency, ω_1, while the light vector, L, is rotating about the same axis at ω_2. In the rotating coordinate system ω_2 is considered stationary and the light vector can be considered to be rotating about the z-axis at an angular velocity of $(\omega_2 - \omega_1)\, t$. This can be likened to a spot of light moving slowly around an axis, such as that seen by a strobe light on a flywheel where the rotation and blinking are not exactly in synchronization. Consequently, the magnetization vector $\vec{M}$ is located in the area between the H_{eff} and L vectors and precesses about the z-axis.

If $|\omega_2 - \omega_1| << \frac{1}{T_1}$ (the magnetic relaxation time), d.c. calculations may be used in evaluating the equations 4,5,6.

Therefore, the differential terms are equal to zero and it is required to solve the resulting equations. Rearranging and regrouping these equations results in the following equations:

$$M_{x'} = S\gamma(H_0 - \omega/\gamma) M_{y'} + M_{x'}^{(0)}$$

$$M_{z'} = -\gamma H_1 S M_{y'} + M_{z'}^{(0)}$$

$$M_{y'} = \gamma H_1 S M_{z'} - \gamma(H_0 - \omega/\gamma) S M_{x'}$$

$$= M_{y'}^{(0)} + \gamma H_1 S M_{z'}^{(0)} - \gamma(H_0 - \omega/\gamma) S M_{x'}^{(0)} - \gamma^2 H_1^2 S^2 M_{y'} - \gamma^2 (H_0 - \omega/\gamma)^2 S^2 M_{y'}$$

$$= \frac{M_{y'}^{(0)} + \gamma H_1 S M_{z'}^{(0)} - \gamma (H_0 - \omega/\gamma) S M_{x'}^{(0)}}{1 + \gamma^2 H_1^2 S^2 + \gamma^2 (H_0 - \omega/\gamma)^2 S^2} \qquad (7)$$

Using the above equation obtained for $M_{y'}$, the solutions for $M_{x'}$ and $M_{z'}$ are as follows:

$$M_{x'} = \frac{(1 + \gamma^2 H_1^2 S^2) M_{x'}^{(0)} + \gamma S (H_0 - \omega/\gamma) M_{y'}^{(0)} + \gamma^2 S^2 H_1 (H_0 - \omega/\gamma) M_{z'}^{(0)}}{1 + \gamma^2 H_1^2 S^2 + \gamma^2 (H_0 - \omega/\gamma)^2 S^2} \qquad (8)$$

$$M_{z'} = \frac{\gamma^2 H_1 (H_0 - \omega/\gamma) S^2 M_{x'}^{(0)} - \gamma H_1 S M_{y'}^{(0)} + [1 + \gamma^2 (H_0 - \omega/\gamma)^2 S^2] M_{z'}^{(0)}}{1 + \gamma^2 H_1^2 S^2 + \gamma^2 (H_0 - \omega/\gamma)^2 S^2} \qquad (9)$$

Next it is required to obtain values for the terms $M_{x'}^{(0)}$, $M_{y'}^{(0)}$, AND $M_{z'}^{(0)}$. This will be accomplished as follows: Following Bell and Bloom,[12] the behavior of the spin system in terms of phenomenological equations for a system of particles of spin 1/2 will be investigated briefly. From there a plausibility type argument will be made to show that the same quantities can be obtained for a spin 1 system. Detailed analysis of this behavior is beyond the scope of this thesis.

Consider the optical effects, in the absence of a magnetic field, of only two Zeeman levels, α and β. If F_i is the pumping rate out of the i th level and a_i is the population of this level, then the net pumping process can be described by the following system of equations:

$$\frac{da_i}{dt} = -a_i P_i + n^{-1} \Sigma a_j P_j \qquad (10)$$

$$\Sigma a_i = A_0 \qquad (11)$$

where n is the number of levels in the $S_{1/2}$ ground state and A_0 in the total population of the sample.

Using equations 10 and 11 the following equations can be written:

$$\frac{dM_z}{dt} = (M_0 - M_z) P_z$$

$$M_z = a_\alpha - a_\beta$$

and by simple mathematics it can be shown that $a_\alpha P_\alpha = a_\beta P_\beta$

In a state of equilibrium $\frac{dM_z}{dt} = 0$

and, by definition

$$M_0 = M_z = a_\alpha - a_\beta$$

solving for M_0

$$M_0 = a_\alpha \left(1 - \frac{P_\alpha}{P_\beta}\right) = \frac{a_\alpha (P_\beta - P_\alpha)(P_\beta + P_\alpha)(a_\alpha + a_\beta)}{P_\beta \quad (P_\beta + P_\alpha)(a_\alpha + a_\beta)}$$

In order to obtain the equation for M_0 cited in the above paper it is only necessary to show that

$$\frac{(P_\beta + P_\alpha)(a_\alpha)}{P_\beta (a_\alpha + a_\beta)} = 1$$

12. W. E. Bell and A. L. Bloom, Phys. Rev. 107, 1559 (1957)

This can be easily shown:

$$a_\alpha (P_\beta + P_\alpha) = (a_\alpha + a_\beta) P_\beta$$

remembering

$$a_\alpha P_\alpha = a_\beta P_\beta$$

rearranging and substituting:

$$\frac{P_\beta + P_\alpha}{P_\beta} = \frac{a_\alpha + a_\beta}{a_\alpha} = \frac{a_\alpha + a_\alpha P_\alpha / P_\beta}{a_\alpha} = \frac{P_\beta + P_\alpha}{P_\beta}$$

Therefore, the following desired equations are obtained:

$$M_z = a_\alpha - a_\beta$$

$$M_0 = \frac{A_0 (P_\beta - P_\alpha)}{(P_\beta + P_\alpha)} \tag{12}$$

In a spin 1 system with levels α, β, γ it is easily shown that

$$a_\alpha P_\alpha = a_\beta P_\beta = a_\gamma P_\gamma \tag{13}$$

And in three levels equally spaced in thermal equilibrium (possibly as a negative temperature) the following relationship between the populations of the levels will be found:

$$a_\beta^2 = a_\alpha a_\gamma \tag{14}$$

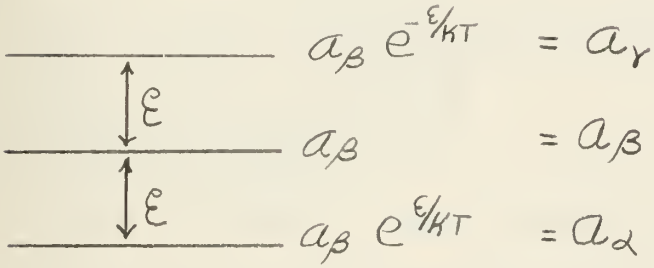

It is plausible that in equilibrium

$$M_0 = M_z = a_\alpha - a_\beta \tag{15}$$

From equation (13), this can be written in the form

$$M_0 = a_\alpha \left(\frac{P_\gamma - P_\alpha}{P_\gamma} \right) = \frac{a_\alpha}{P_\gamma} (P_\gamma - P_\alpha) \tag{16}$$

Moreover from (11) and (14) it is possible to show that

$$a_\alpha(P_\alpha + P_\beta + P_\gamma) = P_\gamma(a_\alpha + a_\beta + a_\gamma)$$

or

$$\frac{a_\alpha}{P_\gamma} = \frac{a_\alpha + a_\beta + a_\gamma}{P_\alpha + P_\beta + P_\gamma} \tag{17}$$

If (17) is substituted in (16) above, there results

$$\mathcal{M}_0 = (a_\alpha + a_\beta + a_\gamma)\left(\frac{P_\gamma - P_\alpha}{P_\alpha + P_\beta + P_\gamma}\right) \tag{18}$$

This clearly is the expression for spin 1 analogous to equation (12) which was expressed for the case of spin 1/2, and the validity of (18) requires only that the spin system be in thermal equilibrium; that is

$$a_\alpha a_\gamma = a_\beta^2$$

Equation (18) holds for all three axes for pumping only, in the absence of all other effects.

By definition $M_{x'}^{(0)} = \mathcal{M}_0 P_{x'} S$

$M_{y'}^{(0)} = \mathcal{M}_0 P_{y'} S$

$M_{z'}^{(0)} = \mathcal{M}_0 P_{z'} S$

Let I_o = intensity of light

Now, the pumping is proportional to the light intensity; therefore

$P_{x'} = K I_o \sin\theta \cos\phi$

$P_{y'} = K I_o \sin\theta \sin\phi$

$P_{z'} = K I_o \cos\theta$

where K = constant of proportionality which need not be evaluated. It is only necessary that the above functions be linear functions of the light intensity.

Therefore,

$$M_{x'}^{(0)} = \mathcal{M}_0 K I_o S \sin\theta \cos\phi \longrightarrow L^{(0)} \sin\theta \cos(\omega_2 - \omega_1)t \tag{19}$$

and likewise;

$$M_{y'}^{(0)} = L^{(0)} \sin\theta \sin(\omega_2 - \omega_1)t \tag{20}$$

$$M_{z'}^{(0)} = L^{(0)} \cos\theta \tag{21}$$

Transform from the rotating coordinate system to the fixed coordinate system by the use of the following equations:

$$M_x = M_{x'} \cos \omega_1 t + M_{y'} \sin \omega_1 t$$
$$M_y = -M_{x'} \sin \omega_1 t + M_{y'} \cos \omega_1 t$$
$$M_z = M_{z'}$$

The high frequency terms are of no interest, therefore all that will be considered are the d.c. and low frequency terms:

$$M_x = M_y = 0$$

$$M_z = \frac{L^{(\omega)} \cos\theta [1 + \gamma^2 (H_0 - \omega/\gamma)^2 S^2] - \gamma H_1 S \sin\theta \sin(\omega_2 - \omega_1)t + \gamma^2 H_1 (H_0 - \omega/\gamma)^2 \sin\theta \cos(\omega_2 - \omega_1)t}{1 + \gamma^2 H_1^2 S^2 + \gamma^2 (H_0 - \omega/\gamma)^2 S^2}$$

The terms of interest are:

$$\gamma H_1 S \sin(\omega_2 - \omega_1)t + \gamma^2 S^2 H_1 (H_0 - \omega/\gamma) \cos(\omega_2 - \omega_1)t$$

The phase angle at resonance is 90 degrees

The phase angle off resonance is $90 + \phi$

where $\phi = \tan^{-1} \frac{\gamma^2 S^2 H_1 (H_0 - \omega/\gamma)}{\gamma S H_1} = \tan^{-1} \gamma S (H_0 - \omega/\gamma)$

define

$$\delta = S(H_0 - \omega/\gamma)$$

therefore $\phi = \tan^{-1} \gamma \delta$

Comments on the above equations:

1. A 60 cycle sweep varies the d.c. term of M_z and for other terms introduces $\omega_2 - \omega_1 \pm 60$ cycles

2. With no sweep (this will be substantiated by experiment)
   a. on resonance: last term equals zero
      diff. freq. equals 90 degrees from straight mixing
   b. off resonance: Phase angle can be computed from the two terms

V. Experimental Apparatus and Procedure

A. Description of Apparatus

The magnetometer consists of three major units, the light source, the absorption cell and the photodetector.

The light source unit consists of a helium lamp, a spherical mirror, a 120mc exciter, a modulator and an oscillator. To obtain a bright pumping light source, the lamp is coupled to the 120mc exciter by two coils. A 140kc signal from the oscillator is amplified and used to grid modulate the 120mc exciter at the resonance frequency. The spherical mirror is used to increase and collimate the pumping light.

The absorption cell contains helium at approximately 0.5 mm of Hg. The helium atoms are continuously excited into a visible but weak discharge by a 30mc exciter again coupled to the absorption cell by coils. This weak discharge provides a source of metastable helium atons which are necessary for the desired transitions. A circular coil connected to a variable frequency oscillator is placed around the absorption cell perpendicular to the ambient magnetic field. The frequency of this r-f magnetic drive oscillator is near that of the light source modulation frequency.

The photodetector unit consists of an Ektron detector and a pre-amplifier.

In operation, light from the bright helium lamp is passed through a lens system to increase the usable pumping light and also through a linear polarizer and quarter wave plate to form circular polarized infra-red light before entering the absorption cell. The light not absorbed in the cell continues through a short focal length lens system and strikes a photodetector contained in the pre-amplifier housing.

The signals from the 140kc oscillator and the r-f magnetic drive oscillator are combined in a mixer unit from which their difference frequency, at a specific phase angle, is obtained. This difference frequency is applied to the vertical input of an oscilloscope. The output signal of the photodetector unit which has the same frequency difference, but a different phase angle, is applied to the horizontal input of the same oscilloscope.

The difference frequency from the mixer is also applied to the vertical input of a reference oscilloscope. The frequency of a reference oscillator, which is equal to the difference frequency, is applied to the horizontal input of the reference oscilloscope. The reference oscilloscope and reference oscillator are used to set up and monitor the frequency difference from the two previously mentioned oscillators.

The apparatus uses regulated power supplies. Two complete supplies are used; one for the 120mc exciter plate voltage and the other for the modulator plate voltage. The plate voltage for the 30mc exciter is supplied by two 45 volt batteries.

Filament power for the modulator, the 120mc exciter and the 30mc exciter is provided by a 6 volt wet cell battery.

Fig. 8 is a schematic diagram of the apparatus. Not included on the diagram is the 60 cycle sweep field unit consisting of a coil, a transformer and a variac. This unit is used to vary the ambient magnetic field when a signal from either the modulated light or the r-f magnetic drive is desired.

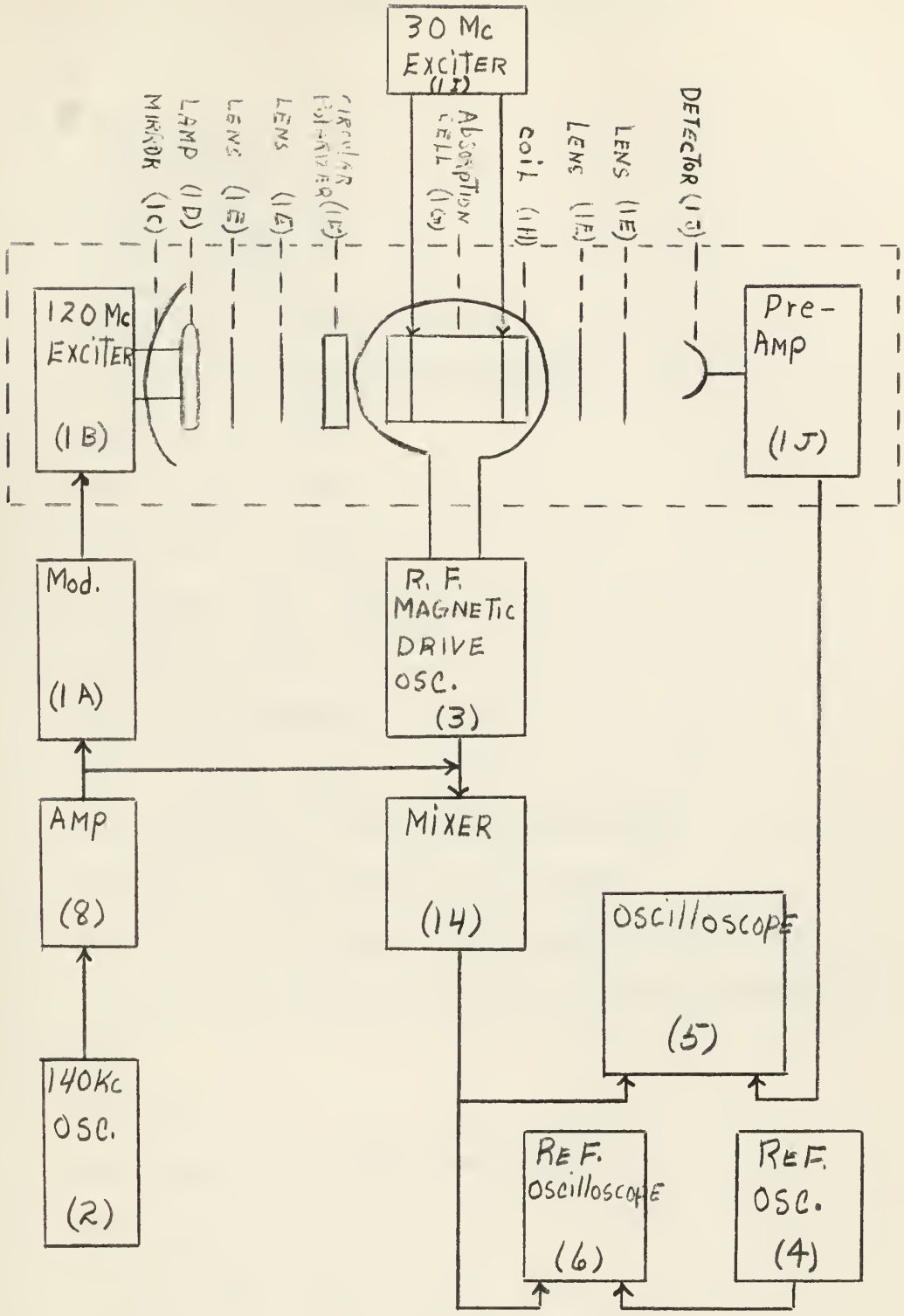

Fig. 8 Schematic Diagram of Apparatus

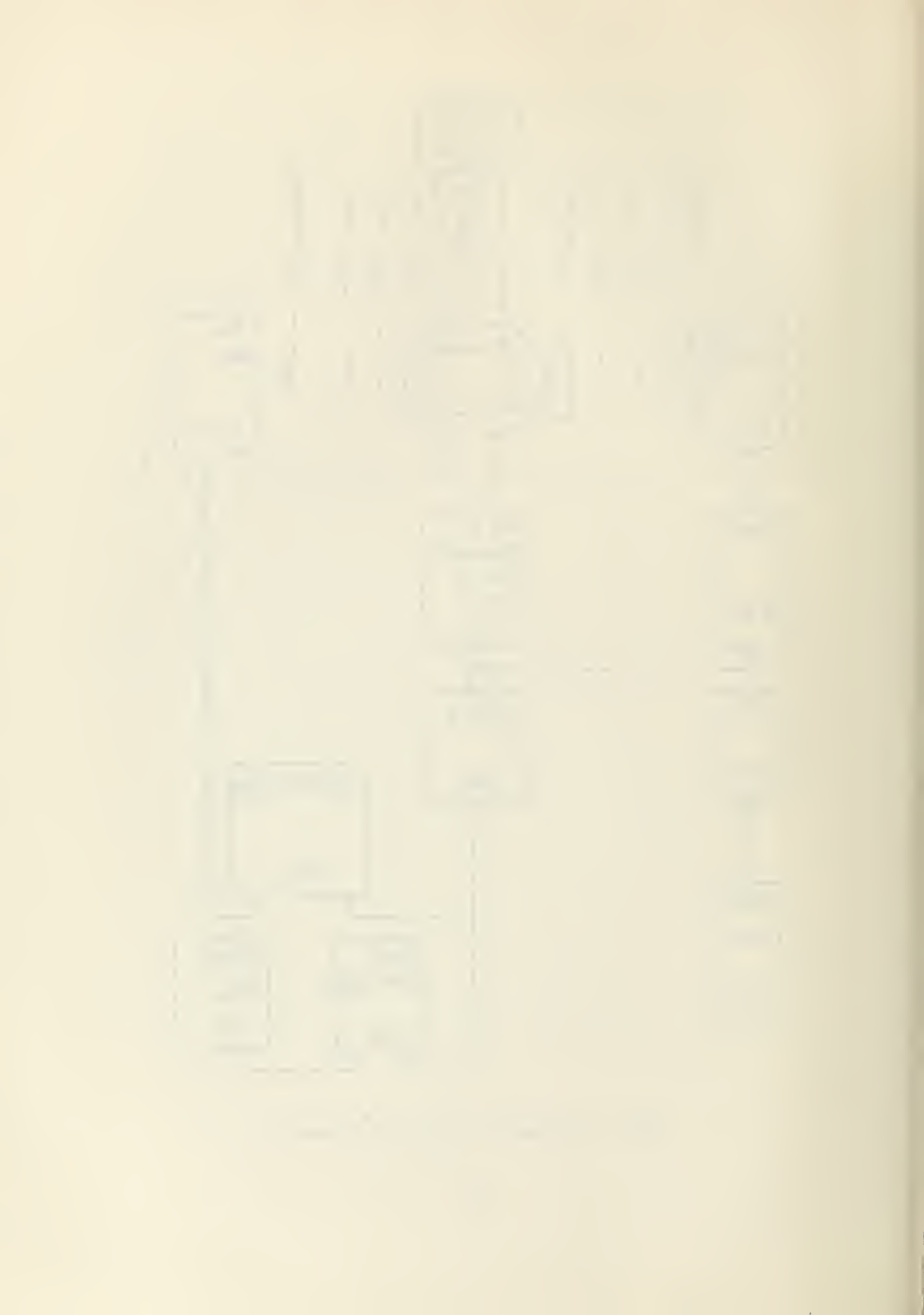

A complete list of the equipment used is given below:

1. Magnetometer Unit

   A. Modulator
   B. 120mc Exciter
   C. Spherical Mirror
   D. Helium Lamp
   E. Fresnel Lenses (4)
   F. Circular Polarizer
   G. Absorption Cell
   H. R-F Coil for Magnetic Drive
   I. 30mc Exciter
   J. Photodetector and Pre-amp Assembly

2. Oscillator, H.P. 204B

3. Oscillator, H.P. 650A

4. Oscillator, H.P. 200CD

5. Oscilloscope, H.P. 130B

6. Oscilloscope, H.P. 310

7. Camera, Oscilloscope

8. Amplifier, H.P. 450A

9. Auto Transformer, Variac, Gen. Radio, W5MT

10. Transformer, Special Services, Type S-65

11. Coil for 60 cycle sweep to vary magnetic field

12. 60 cycle phase splitter to position signal on oscilloscope

13. Mixer

14. Telsa Coil

15. Power Supply, K. H. Model UHR-220 (2)

16. Power Supply Filter

17. 45 volt Burgess Battery (2)

18. 6 volt wet cell Battery and Battery Charger

B. Measurement Procedure

Bell and Bloom in private correspondence have stated that the index of modulation decreases very rapidly with an increase in frequency. The index of modulation obtained at the frequency corresponding to the earth's magnetic field of approximately 50,000 gamma was very small. This resulted in a barely discernible modulated light signal. Therefore, in order to optimize the conditions under which the experiments were performed it was decided to operate the apparatus in a magnetic field of about 5000 gamma.

The helium magnetometer was placed at the center of a Helmholtz coil system in a "magnetically clean" building in order to be in a homogeneous magnetic field. The field current of the coils was adjusted so that the earth's magnetic field was partially cancelled out leaving a residual magnetic field of approximately 5000 gamma. At this setting, the required frequency for the experiments was 140kc.

Prior to performing the experiments to verify the expected phase change of the difference frequency signal, three experiments were made to establish that the equipment was operating satisfactorily and the desired signals were large enough to work with and to be viewed on an oscilloscope.

The first experiment consisted of obtaining a signal from the r-f magnetic drive only. The magnetometer was positioned so that the light beam was parallel to the magnetic field. The 60 cycle sweep field was placed parallel to the magnetic field and near the absorption cell in order to change the total magnetic field at a 60 cycle/sec. rate. The helium lamp was not modulated at this time, but made as bright as possible by tuning the 120mc exciter. The frequency of the r-f magnetic

drive was set at 140kc. The output of the photodetector unit was applied to the vertical input of an oscilloscope. A voltage proportional to the 60 cycle sweep field was applied to the horizontal input of the same oscilloscope. The signal pattern from the r-f magnetic drive is reproduced in Fig. 9. This pattern will be referred to as the r-f drive signal.

The second experiment consisted of obtaining a signal by modulating the helium light source only. This time the magnetometer was positioned so that the light beam was perpendicular to the ambient magnetic field. The same procedure was followed concerning the use of the 60 cycle sweep field. It was found that only a very small sweep field was required to obtain the modulated light signal. The signal (Fig. 10) obtained was not as large as that from the r-f magnetic drive, but was large enough to work with. The signal to noise ratio of both experiments was large enough so that there was no difficulty in obtaining workable signals.

The third experiment consisted of obtaining the signals from both the r-f drive and the modulated light source. The magnetometer was positioned so that the light beam and the ambient magnetic field were at approximately a 45 degree angle. This angle was selected empirically so that signals were obtained from both the r-f drive and the modulated light. The light was modulated at 140kc. and the r-f drive signal frequency was 141kc. The two signals were then displayed on the oscilloscope (Fig. 11). The frequency of the r-f drive was changed until the two signals beat together (Fig. 12). A frequency setting was obtained at which the signals "locked" and held over a period of time. This signal is shown in Fig. 13.

The main experiments to verify the phase change were then performed. The experiments consisted of setting and maintaining a specific frequency difference between the modulated light source frequency and the r-f magnetic drive frequency. During these experiments the 60 cycle sweep field was turned off. The modulated light frequency was maintained at 140kc. and the r-f drive frequency was set above and below the fixed frequency by 20, 50, 100, 200, 500, 1000, and 1500 cycles/sec. At each setting of the r-f drive frequency the field current of the Helmholtz coils was varied manually thus "sweeping" the magnetic field through the values associated with the two frequencies. The output of the photodetector unit was applied to the horizontal input of the oscilloscope. The frequencies from the two oscillators were mixed together and the difference frequency applied to the vertical input of the oscilloscope. The phase difference and phase change as predicted by the theory of radiofrequency mixing was observed and is described in the next section.

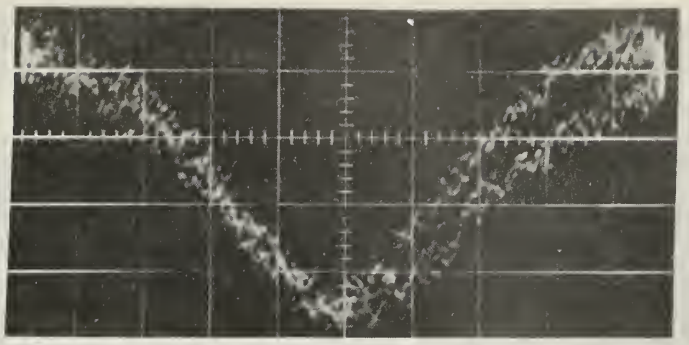

Fig. 9 R-F Magnetic Drive Signal as Displayed on an Oscilloscope
Scale: Vertical 0.1 volt/div Horizontal 1 volt/div

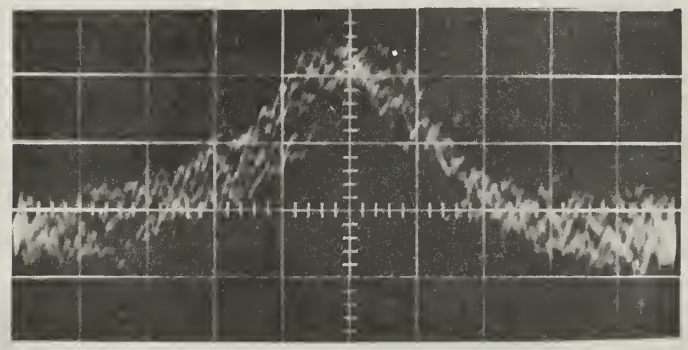

Fig. 10 Modulated Light Resonance Signal as Displayed on an Oscilloscope
Scale: Vertical 0.1 volt/div Horizontal 1 volt/div

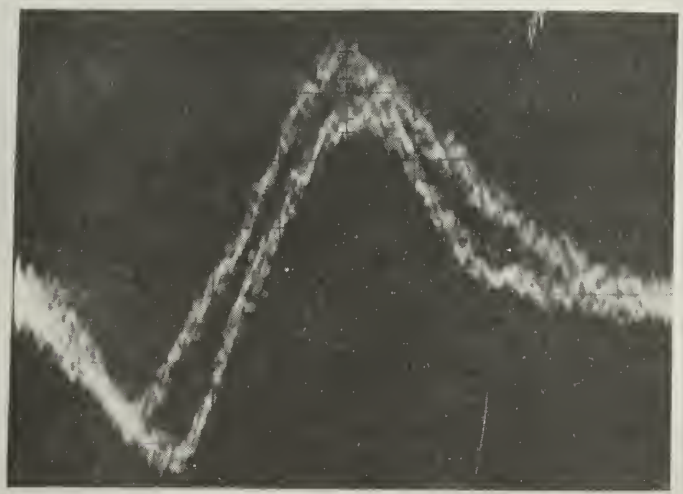

Fig. 11 Oscillogram of both Signals
Scale: Vertical 0.2 v/div
Horizontal 1 v/div

Fig. 12 Oscillogram of Beat Frequency
Scale: Vertical 0.2 v/div

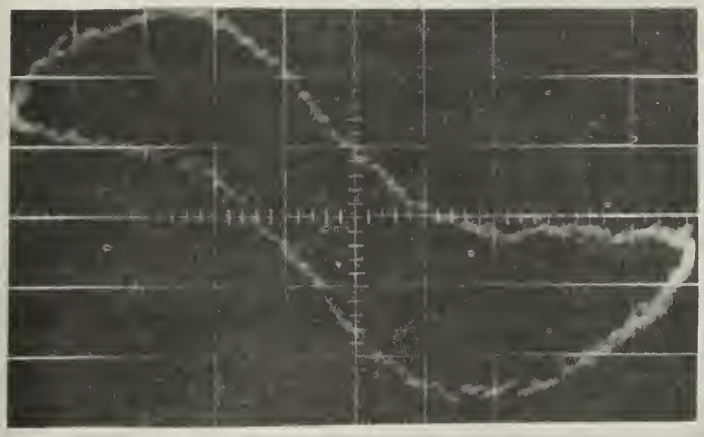

Fig. 13 Oscillogram of "Locked" Signals
Scale: Vertical 0.2 v/div
Horizontal 1 v/div

VI. Results and Conclusions

A. Results

The purpose of this work was to obtain information concerning the phase characteristics of the frequency signal, thus verifying the theory. The data obtained bear out the theory. It would appear that this property of the radiofrequency mixing system would enable one to build a helium magnetometer closed loop oscillator which would be able to continuously measure the variations of the earth's magnetic field. Two such systems are proposed in part C of this section.

The results are shown in Figs. 15 - 21. As can be seen from the oscillograms, there is a definite phase shift of the output signal as the magnetic field is swept through the frequency difference. The limiting frequency differences were dictated by the observable oscilloscope presentation. The only criteria followed in determining the frequency was the line width of the resonance curve. As long as both signals were within the line width the expected phase change should be observable. Above a 1500 cycles/sec. frequency difference the phase change could be observed, but the scope presentation was too noisy for proper evaluation. The oscillators were not stable enough to hold a frequency difference of less than 20 cycles/sec.

The oscillograms were taken at the positions as illustrated in Fig. 14. The three pictures in the left hand column of each figure show the three positions that were photographed. For this set of pictures the r-f magnetic drive frequency was set higher than the light modulating frequency. The pictures in the right hand column were of the same three positions except now the r-f magnetic drive frequency was set lower than the light modulating frequency.

Initially the current in the Helmholtz coil system was set so that the resonance frequency was higher than either the light modulating or r-f magnetic drive frequency. Then the current in the coils was increased. This increased the opposing magnetic field resulting in a decrease in the ambient magnetic field. With a decrease of the ambient magnetic field, the resonance frequency decreased. This, in effect, swept the resonance frequency through the fixed frequency difference. As can be observed from the following oscillograms, the phase of the output signal was different depending upon the location of the resonance frequency with respect to the fixed frequency difference.

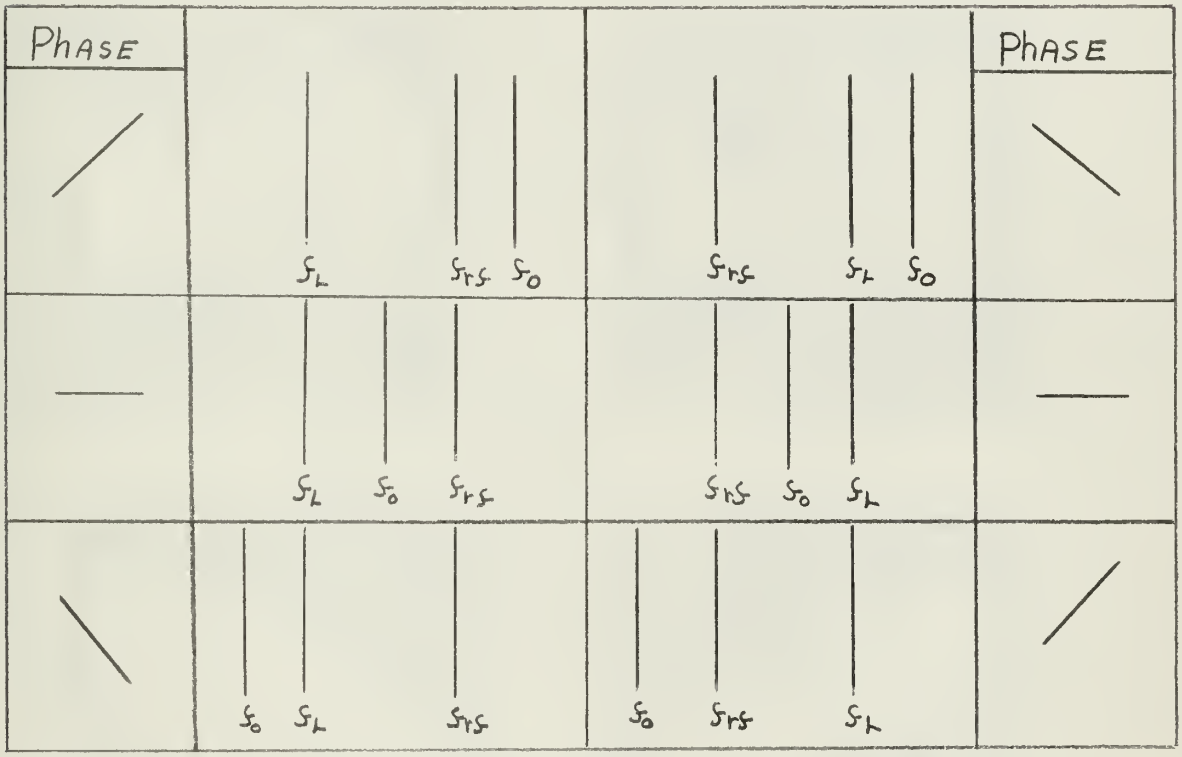

Note: frequency increases to the right

f_o = resonance frequency
f_1 = light modulating frequency
f_{rf} = r-f magnetic drive frequency

Fig. 14 Diagram of Positions Photographed

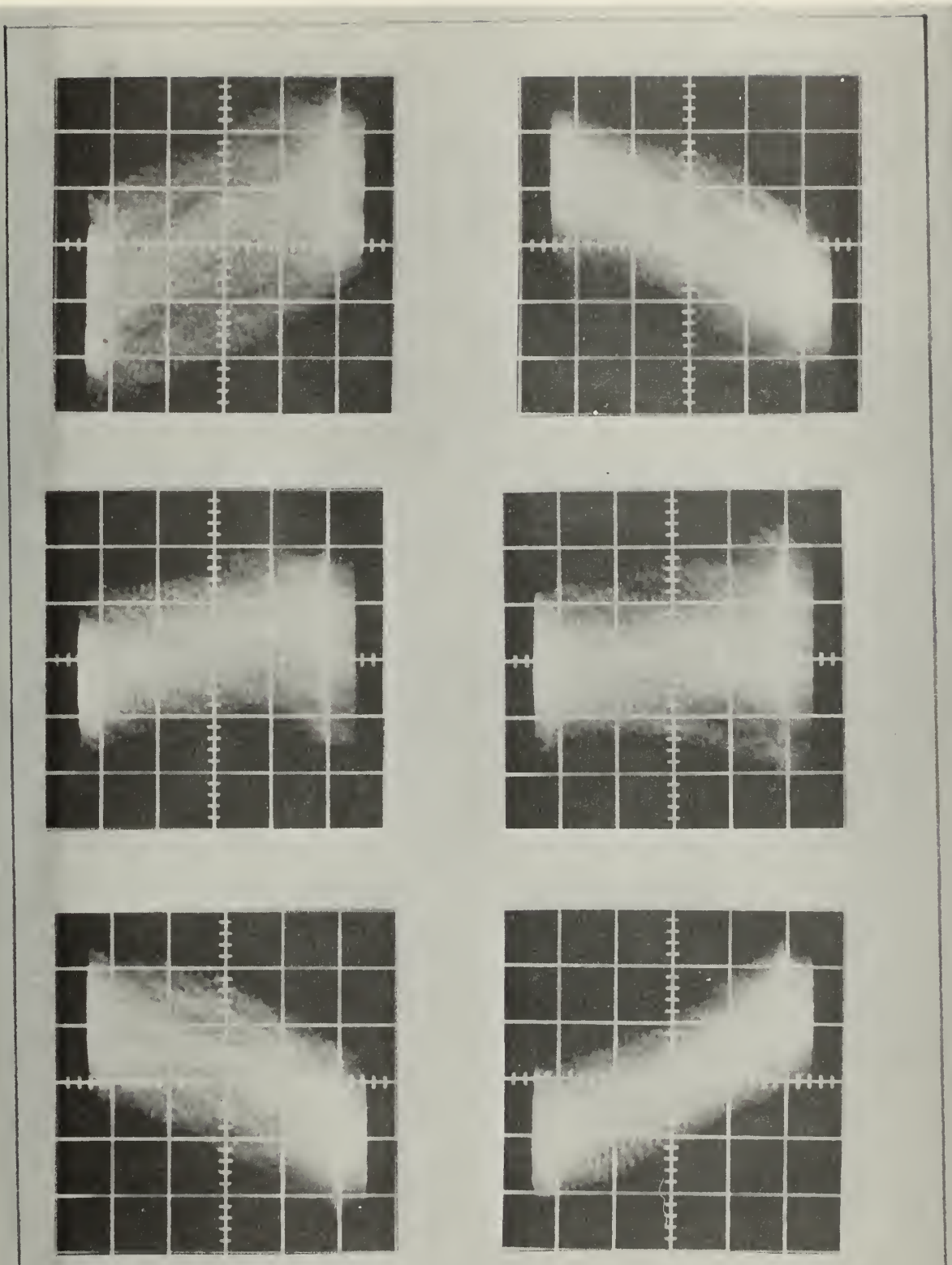

Fig. 15 Oscillograms of Phase Difference for freq. difference of 1500 cycles

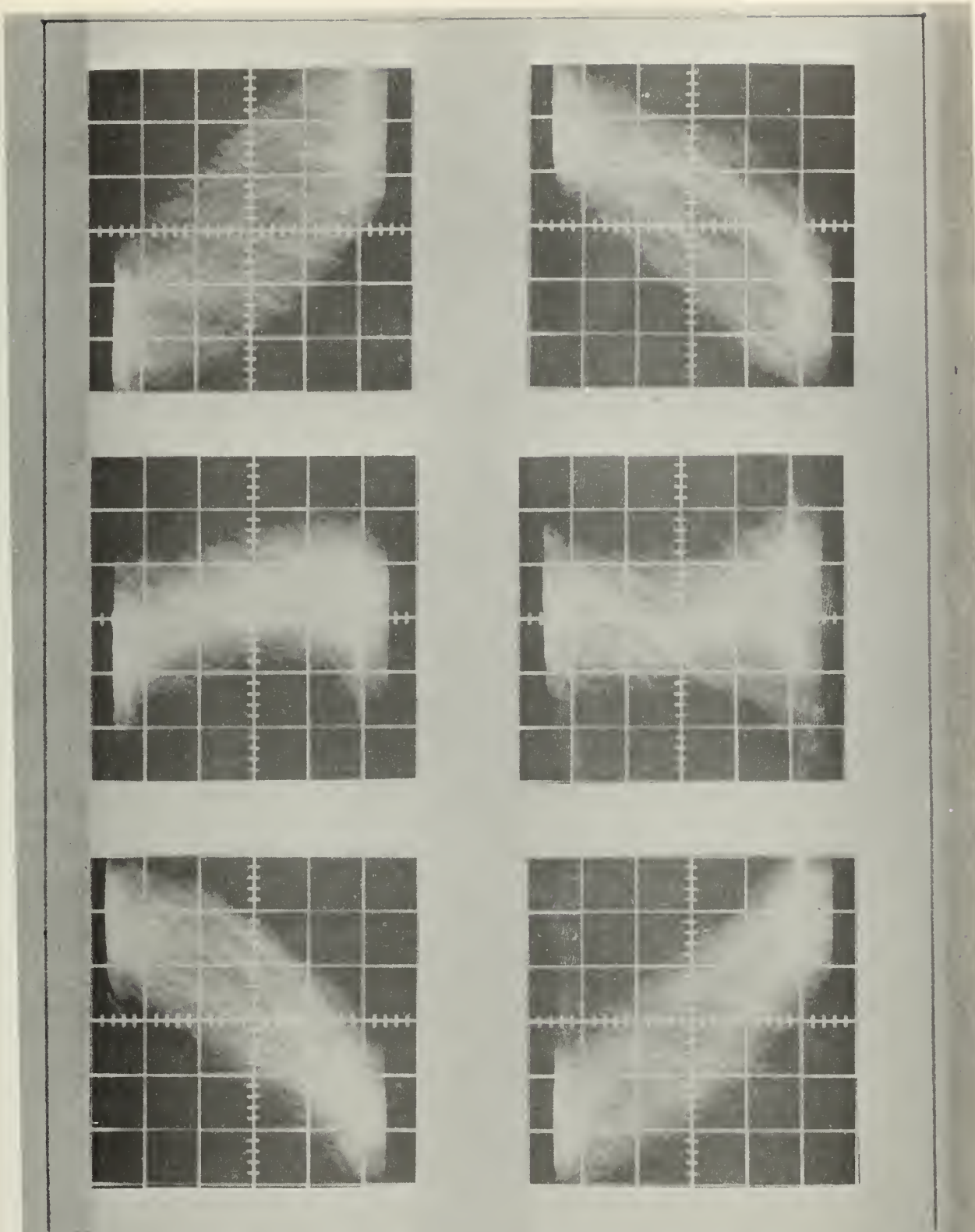

Fig. 16 Oscillograms of Phase Difference for freq. difference of 1000 cycles

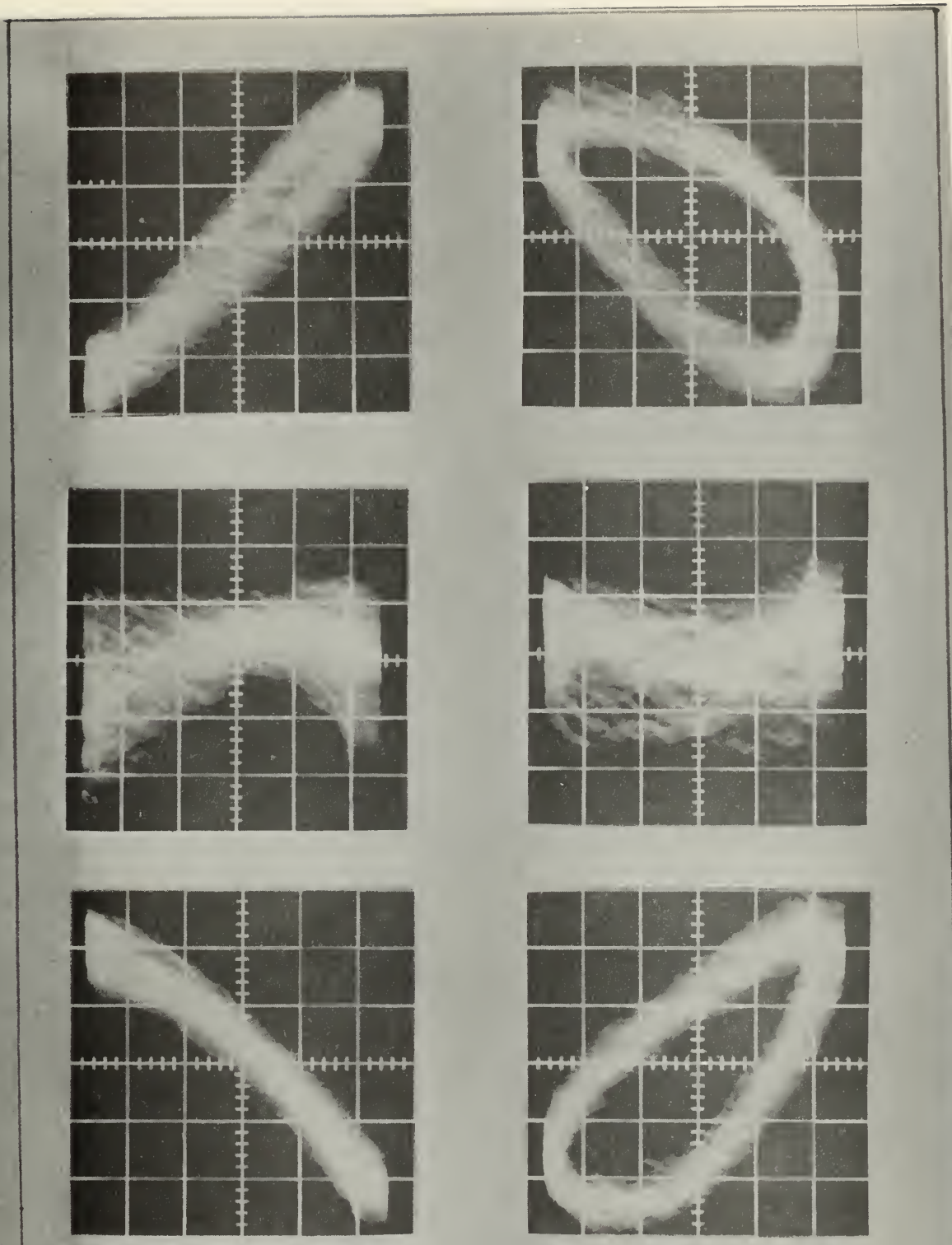

Fig. 17 Oscillograms of Phase Difference for freq. difference of 500 cycles

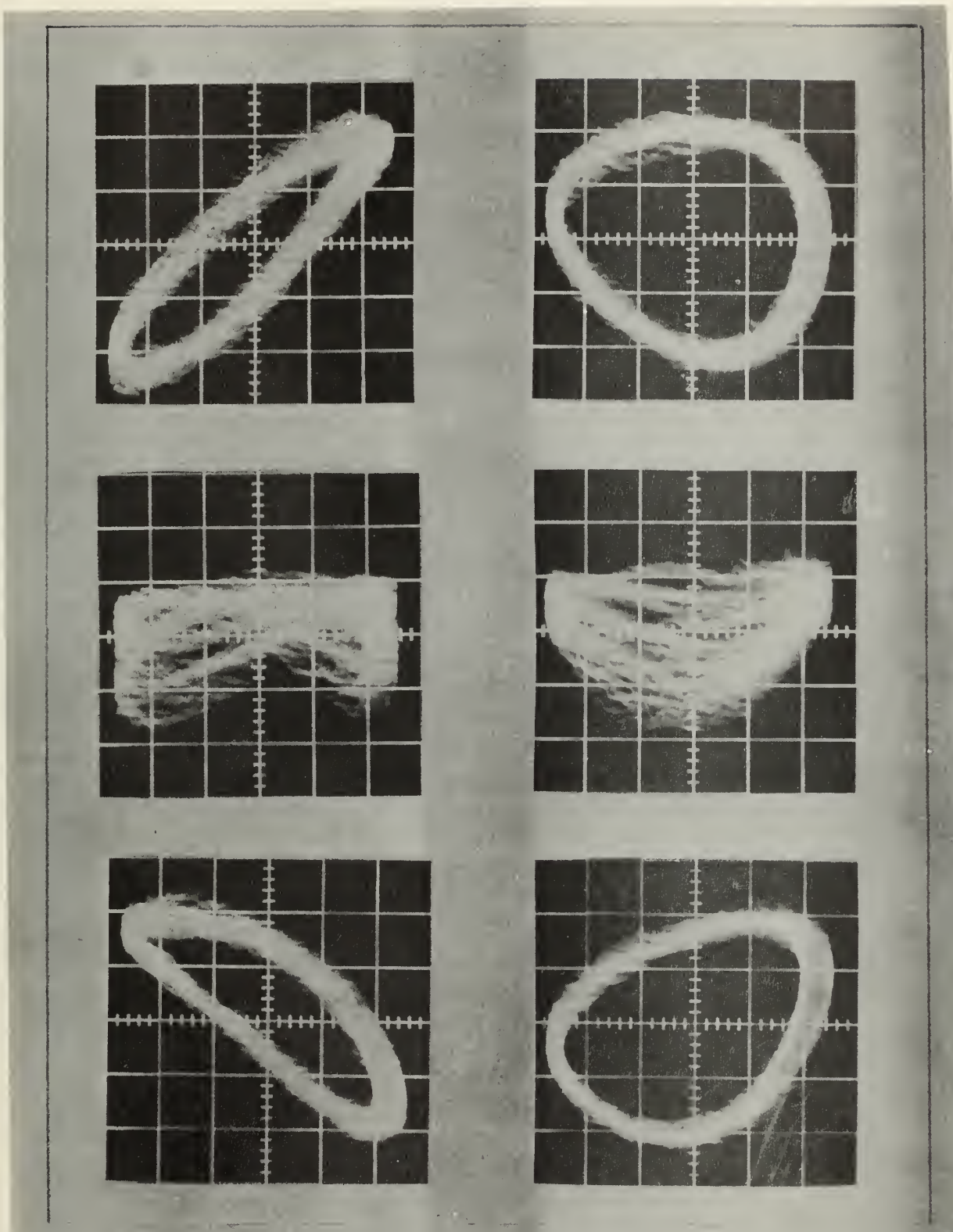

Fig. 18 Oscillograms of Phase Difference for freq. difference of 200 cycles

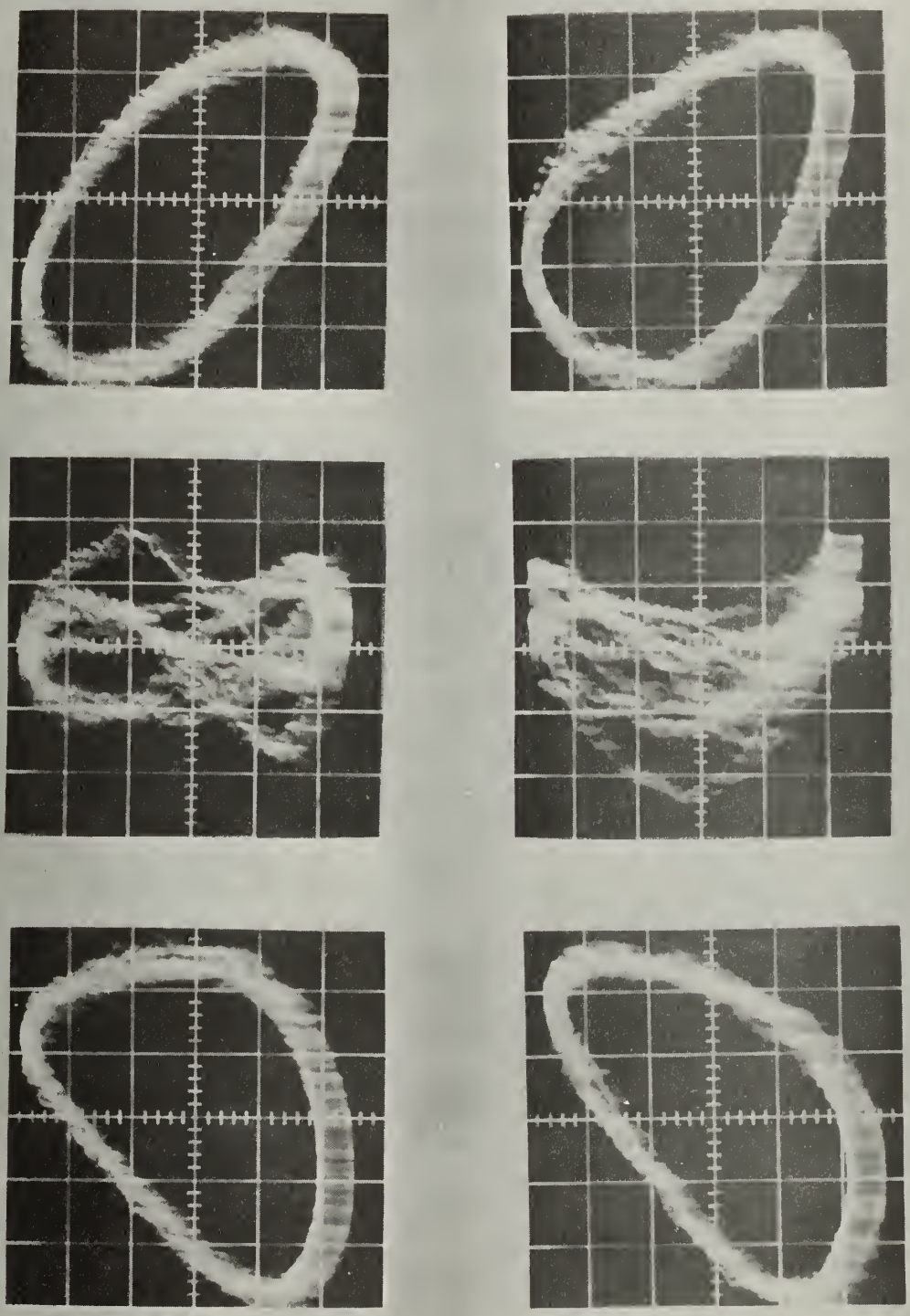

Fig. 19 Oscillograms of Phase Difference for freq. difference of 100 cycles

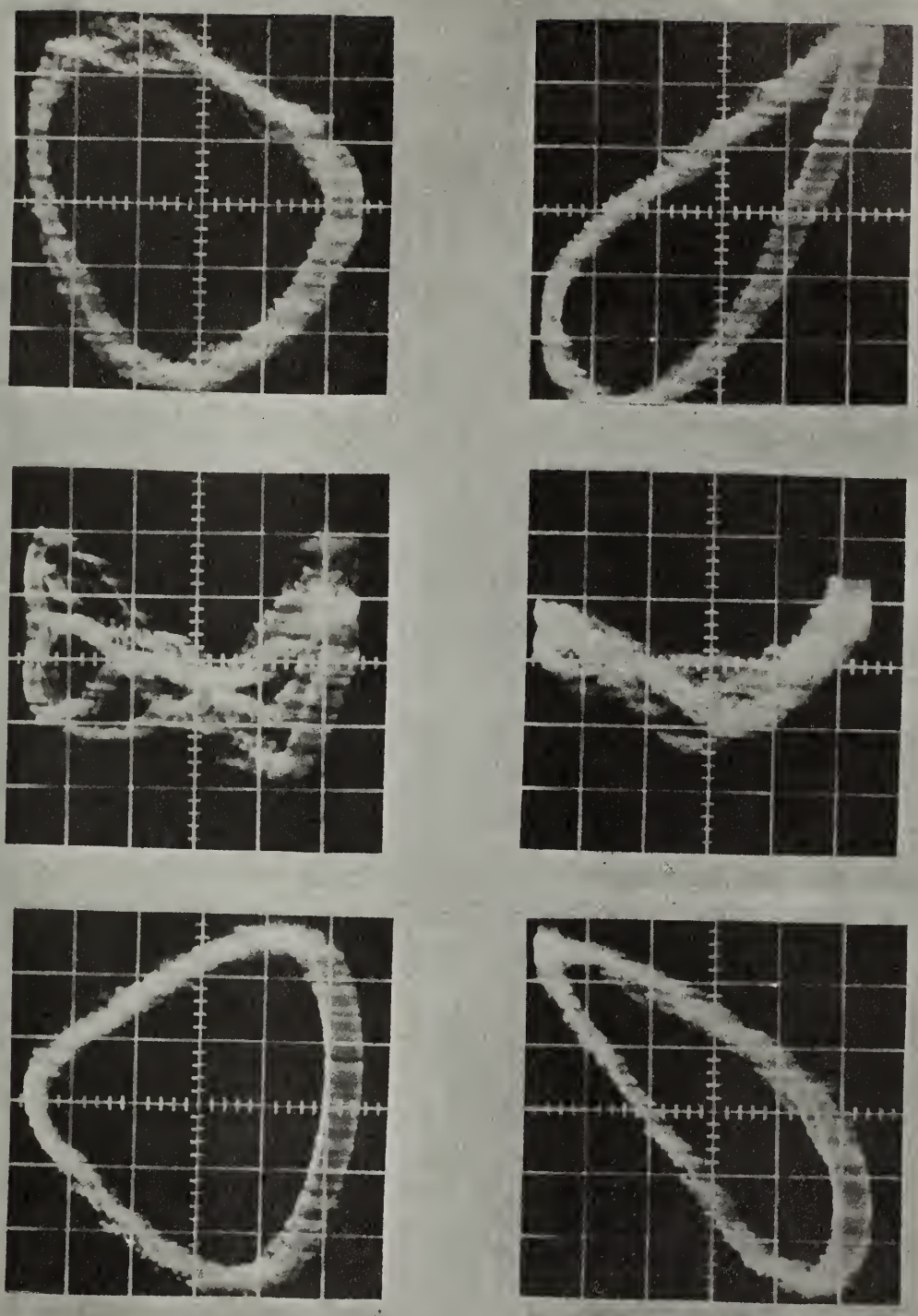

Fig. 20 Oscillograms of Phase Difference for freq. difference of 50 cycles

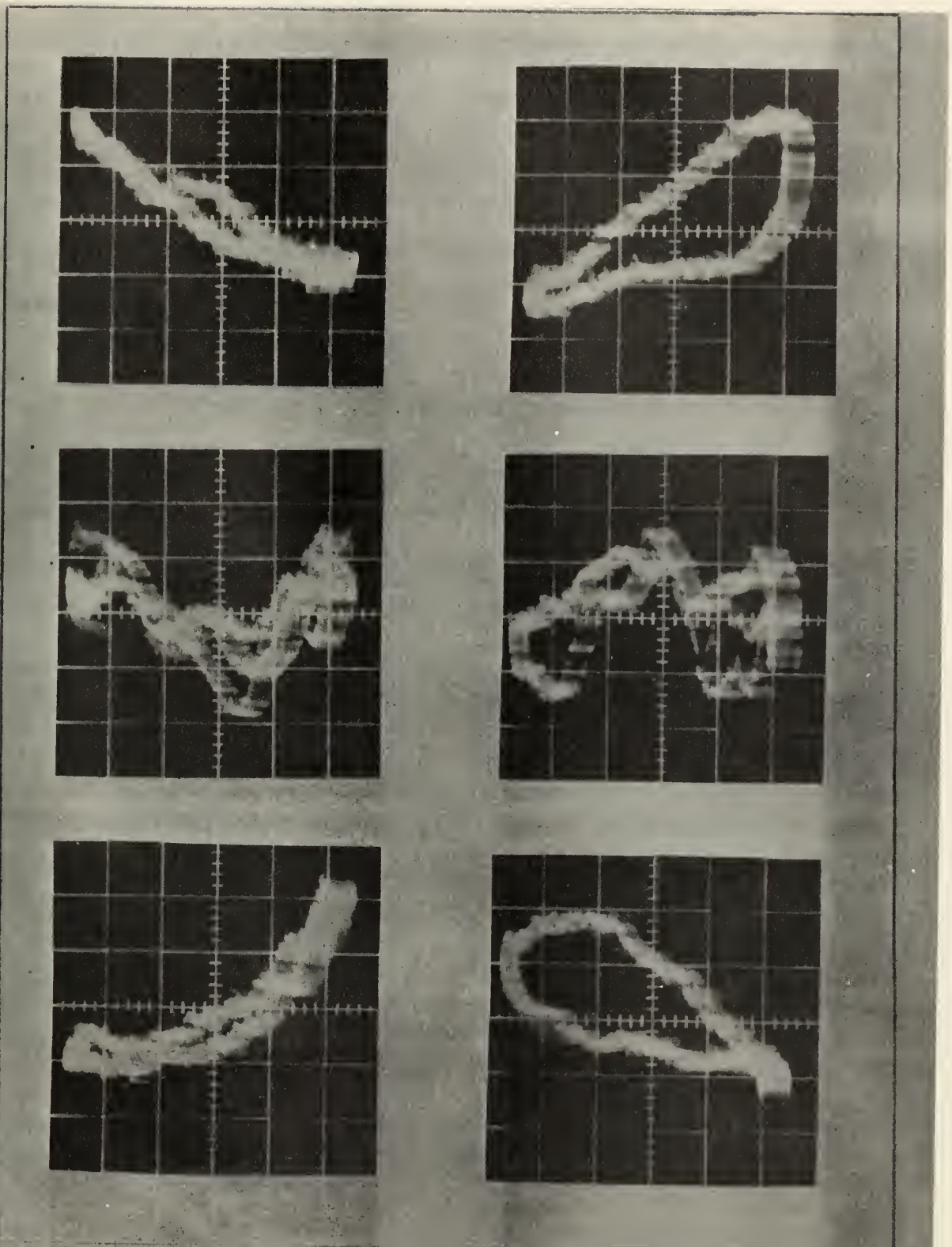

Fig. 21 Oscillograms of Phase Difference for freq. difference of 20 cycles

B. Limitations of Experimental System

During this investigation, no particular emphasis was placed on accuracy provided the results obtained could be clearly associated with the changes in the ambient field. The actual measurements confirmed the fact that the theoretical concept was verified.

Several modifications could be made to improve the accuracy of the equipment:

1. Environment

The apparatus was installed in a building which contained a variable 60 cycle sweep field and equipment which caused magnetic interference. A magnetically-clean environment would eliminate these problems. Test equipment had to be placed at a distance from the magnetometer to prevent interference with its operation. It is believed that the test equipment should be placed in a shielded enclosure to minimize its interference.

2. Packaging

The system components used were bulky and inadequately shielded. This added to the magnetic clutter and provided numerous sources of noise. Complete shielding of all of the components of the system would eliminate the above mentioned troubles.

3. Grounding and cable connecting system

Open leads and insufficient grounding of all components caused considerable trouble by picking up and conducting extraneous frequencies. The use of shielded cables and a common grounding system for all components of the magnetometer, power supplies, and test equipment would decrease the pick up and noise.

4. Helium Lamp

The helium lamp used was of a "wasp" configuration. The reason for this shape was the belief that the helium in the narrow center section would produce a very bright light and a stronger light beam would result. It was found that a stronger beam could be obtained when one of the larger sections of the lamp was used. The position of the helium lamp in its holder affected the performance of the 120mc exciter and the intensity of light. It was necessary to adjust the position of the lamp frequency for vibrations would loosen it and cause the light intensity to decrease resulting in no obtainable light modulating signal. A lamp with attached electrodes would aid in maintaining the correct lamp position. Difficulty was experienced in modulating the helium light at 1.4mc/s. The light could be modulated at 1.4mc, but with a very low index of modulation. With a low index of modulation it was not possible to obtain a light modulating signal that was strong enough to perform the experiments. It is believed that experiments should be performed on the helium lamp to determine whether any buffer gas added to the helium would quench the helium so that a higher index of light modulation could be obtained for high modulating frequencies.

C. Proposed Closed Loop Oscillator Systems

An experimental closed loop oscillator system is shown in Fig. 22. The two frequencies could be set on either side of the resonance curve with one of the frequencies fixed and the other capable of being changed. When the ambient magnetic field changes the phase of the output signal would change. This phase change would be detected in a phase detector. The output of the phase detector would then change the frequency of one of the oscillators, thus repositioning the frequency difference about the resonance frequency. The amount of frequency change necessary to reposition the difference frequency about the resonance frequency thus indicating the change of the ambient magnetic field.

In the helium system, the conversion ratio is 28 cycles per gamma. Therefore, if the two frequencies were centered about the mean ambient field with a frequency difference of approximately 1000 cycles, the gamma difference would be approximately 285. This would adequately take care of the normal daily magnetic field variations. The only possible weakness of the system would be the occasion when the magnetic field received an extreme perturbation and caused the fixed frequency and the resonance frequency to coincide.

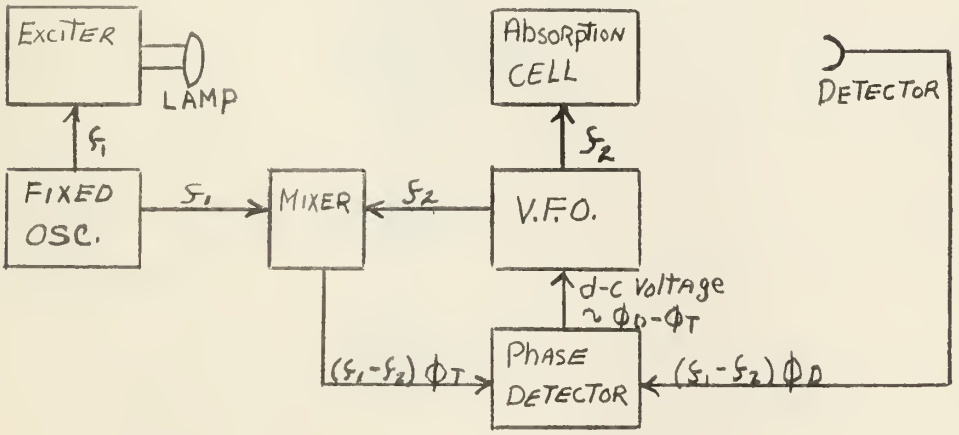

Fig. 22 Proposed Experimental Closed Loop Oscillator

A second system for a closed loop oscillator is shown in Fig. 23. This is a double side band, suppressed carrier system. By this method a fixed frequency difference can be maintained. Whenever the resonance frequency changes due to a change in the ambient magnetic field, the fixed difference frequency is positioned about the new resonance frequency. The shift of frequency which is required to reposition the difference frequency will indicate the change in the ambient magnetic field.

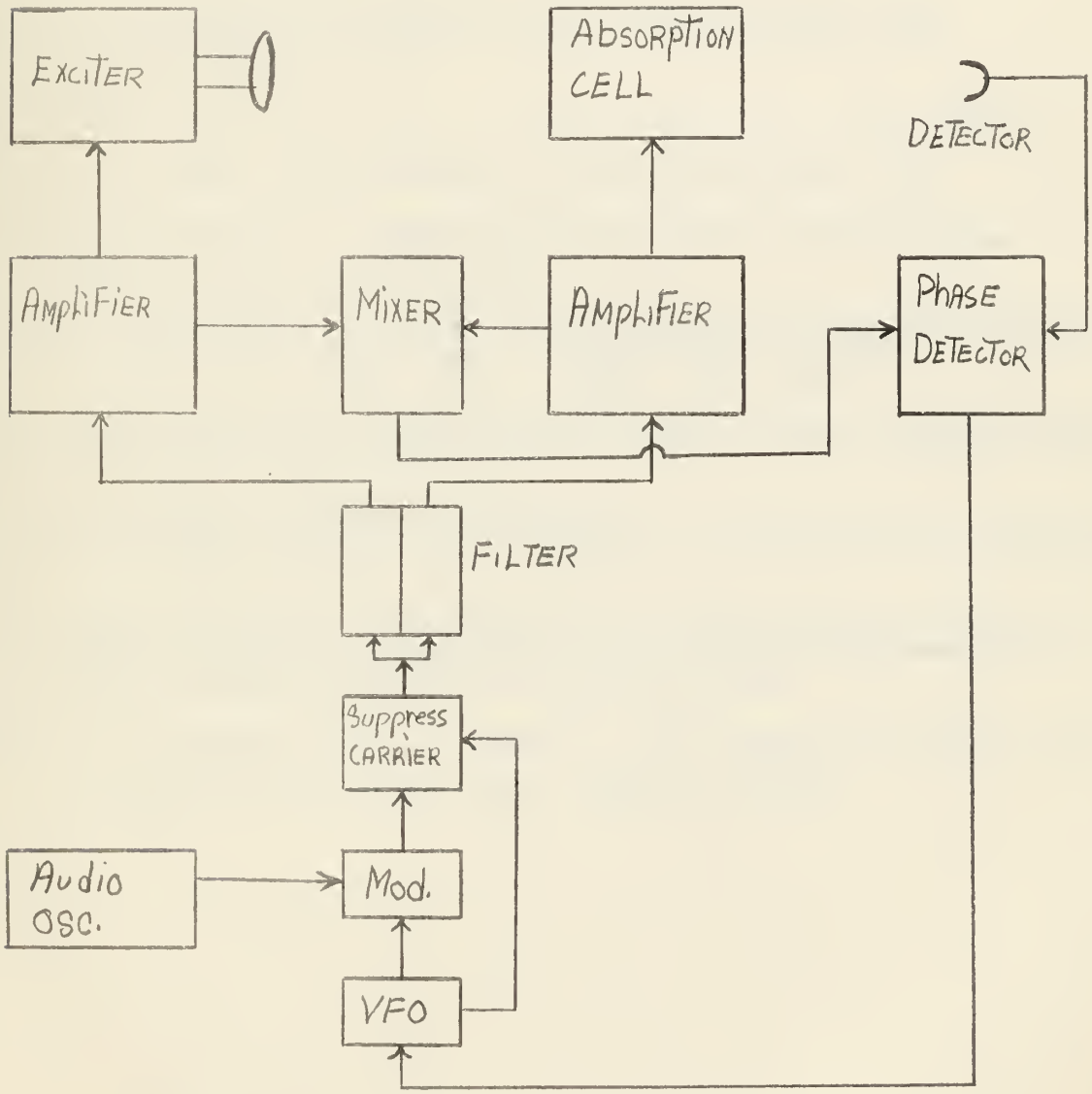

Fig. 23 Proposed Suppressed Carrier System

BIBLIOGRAPHY

1. Max Born, Atomic Physics 4th Edition, Hafner Publishing Company, 1946

2. L. B. Loeb, Atomic Structure, John Wiley and Sons, 1938

3. C. S. Cook, Modern Atomic and Nuclear Physics, D. Van Nostrand Company, 1961

4. L. S. Schearer, The Metastable Helium Magnetometer, Texas Instruments Incorporated, 1960

5. R. G. Aldrich, A Helium Magnetometer That Utilizes Light Modulation, Thesis, 1961

6. M. E. Packard, The Method of Nuclear Induction, Thesis, 1949

7. A. L. Bloom, Optical Pumping, Scientific American, 1960

8. W. E. Bell and A. L. Bloom, Optically Driven Spin Precession, Phys. Rev. Ltrs. 6, 280, (1961)

9. W. E. Bell and A. L. Bloom, Optical Detection of Magnetic Resonance in Alkali Metal Vapor, Phys. Rev. 107, 1559, (1957)

10. A. L. Bloom and W. E. Bell, Radiofrequency Mixing in Optical Pumping Experiments, Varian Associates

11. A. L. Bloom, Principles of Operation of the Rubidium Vapor magnetometer, Applied Optics, Vol. 1, No. 1, 1962

12. F. D. Colgrove and P. A. Franken, Line Shape Effects in the Optical Pumping of Helium, Proceedings of the Ann Arbor Conference on Optical Pumping, University of Michigan, 1959

13. F. D. Colegrove and P. A. Franken, Optical Pumping of Helium in the $^3S_1$ Metastable State, Phys. Rev. 119, 680, (1960)